

# $\pi$ -Coordinated Arene Metal Complexes and Catalysis

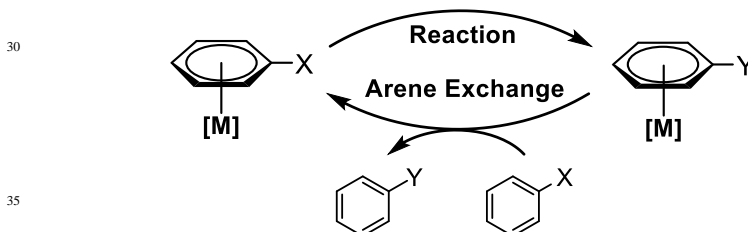
James W. Walton<sup>a\*</sup> and Luke A. Wilkinson<sup>b\*</sup>

DOI: 10.1039/b000000x [DO NOT ALTER/DELETE THIS TEXT]

5 Metal complexes formed from  $\pi$ -coordination of aromatic groups to metal centres may undergo reactions at the coordinated arene that do not occur for the unbound arene. Upon completion of such reactions, the coordinated arene product can be liberated from the metal complex by thermal or photolytic methods. A catalytic approach can also be envisaged in which  
10 the arene transiently  $\pi$ -coordinates to the metal centre, reacts and then undergoes arene exchange for further starting arene. The significant challenge to this catalytic approach is to balance reactivity with arene exchange. In this review, we summarise the synthesis and reactivity of  $\pi$ -arene metal complexes. We go on to discuss the features of arene  
15 exchange and conclude with a comprehensive review of catalytic reactions proceeding via  $\pi$ -arene intermediates.

## 1 Introduction

Catalysis is without doubt one of the major fields of research in chemistry. The discovery of new, effective catalysts has fuelled industry and transformed the world  
20 (Haber-Bosch, Ziegler-Natta, Wilkinson etc.). With the award of no fewer than four Nobel Prizes in this area since the turn of the millennium, it is easy to argue the continual relevance of this discipline. There are many different mechanisms by which efficient homogeneous catalysis is known to occur. One particularly promising, yet relatively unexplored, catalytic mechanism emerging in the literature  
25 is that of catalysis via  $\pi$ -arene metal complex intermediates.  $\pi$ -Coordination to certain metal complexes leads to increased reactivity of the bound arene. Upon reaction, the  $\pi$ -bound product can undergo arene exchange, resulting in reactions that are catalytic in activating metal (Scheme 1).



**Scheme 1:** General mechanism for catalysis via  $\pi$ -arene intermediates.

Despite its apparent simplicity, developing a catalytic cycle that is applicable to  
40 various chemical transformations is an ongoing challenge, due to the requirement for both reaction and arene exchange to proceed under the same conditions. That said, there is a growing number of catalytic reactions in which  $\pi$ -arene intermediates have been identified, showing the viability of this approach. This review chapter

describes the advances towards catalysis through an arene exchange mechanism. We focus on the critical stages of the cycle. The first section briefly covers the synthesis of metal-arene complexes, the scope, limitations and indirect routes towards formation, as well as some recent, thought-provoking examples. The second section explores reactions of  $\pi$ -coordinated arenes, using stoichiometric activating metal complex. The third section investigates the mechanism of, and factors that affect, the arene exchange processes, before the concluding section showcases examples wherein the cycle in Scheme 1 has been successfully realised.

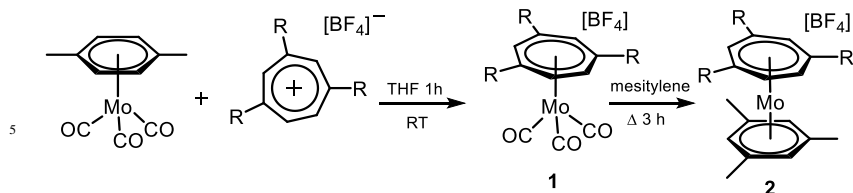
## 2 Synthesis of metal-arene $\pi$ complexes

There are a plethora of  $\pi$ -arene-metal complexes reported in the literature and the syntheses of examples from groups 6-8 of the periodic table have been reviewed previously.<sup>1</sup> This section seeks to summarise recent examples from groups 6-8 and discuss  $\{(\eta^6\text{-arene})\text{M}\}$  complexes from groups 9 and 10. Although  $\pi$ -arene complexes of group 4 and 5 metals exist,<sup>2-9</sup> in the interest of brevity, this review will not cover these species in detail. To the authors' knowledge, there have been no reports of  $\pi$ -arene complexes of the coinage metals Ag and Au, however, a very recent contribution describes the first synthesis and isolation of  $\{(\eta^6\text{-arene})\text{Cu}^{\text{I}}\}$  complexes of benzene and hexamethylbenzene, stabilised by a silylene ligand.<sup>10</sup>

### 2.1 Group 6: Chromium and molybdenum

Perhaps the most numerous type of  $\pi$ -arene-metal complexes are those of the form  $[(\eta^6\text{-arene})\text{M}(\text{CO})_3]$  (where M = Cr or Mo). The synthesis of these species generally occurs via thermolysis of  $[\text{M}(\text{CO})_6]$  in the presence of the arene under inert conditions, or by arene exchange from an initial  $[(\eta^6\text{-arene})\text{M}(\text{CO})_3]$  complex (usually naphthalene or benzene).<sup>11</sup> This latter technique is particularly useful as it is often not possible for a direct complexation from  $[\text{M}(\text{CO})_6]$ , particularly when M is Mo and/or electron poor arenes (e.g.,  $\text{C}_6\text{H}_5\text{NO}_2$ ) are used.<sup>12</sup> In some cases, it is more feasible to go via an  $[\text{L}_3\text{M}(\text{CO})_3]$  intermediate (where L =  $\text{NH}_3$ , pyridine, MeCN). The synthesis of  $[(\eta^6\text{-arene})\text{Cr}(\text{CO})_3]$  complexes has been achieved from  $[\text{Cr}(\text{CO})_6]$  using a continuous flow system, with short reaction times (15 mins), good yields (>70%) and on a gram scale; however the scope for this process remains limited, reflecting the synthetic difficulties associated with electron poor arenes.<sup>13</sup> Chiral arene complexes of  $\{\text{Cr}(\text{CO})_3\}$  have also been extensively studied.<sup>14</sup> Although chirality is often generated via *ortho*-metallation of a monosubstituted  $\eta^6$ -bound arene (e.g.,  $[(\eta^6\text{-C}_6\text{H}_5\text{OMe})\text{Cr}(\text{CO})_3]$ ), arenes bearing chiral sugars have also been directly complexed to the metal centre.<sup>15,16</sup>

In general, molybdenum complexes undergo arene exchange more readily than their chromium counterparts. Indeed, Kündig and co-workers reported that it was possible to synthesise a range of  $[(\eta^6\text{-arene})\text{Mo}(\text{CO})_3]$  complexes in excellent yields from  $[(\eta^6\text{-C}_6\text{H}_6)\text{Mo}(\text{CO})_3]$  at room temperature with the addition of a weak Lewis base, such as THF.<sup>12</sup> All complexes were obtained in high yields after 2 hours, however the scope was limited and excluded electron deficient arenes. To overcome this, Pampaloni employed  $[(\text{DMF})_3\text{Mo}(\text{CO})_3]$  as a synthetic intermediate to access electron-deficient arene complexes,  $[(\eta^6\text{-C}_6\text{H}_5\text{F})\text{Mo}(\text{CO})_3]$  and  $[(\eta^6\text{-C}_6\text{H}_5\text{CF}_3)\text{Mo}(\text{CO})_3]$  in moderate yields.<sup>17</sup> It has also been possible to decorate the  $\{\text{Mo}(\text{CO})_3\}$  fragment with tropylium cations to generate  $[(\eta^7\text{-C}_7\text{H}_4\text{R}_3)\text{Mo}(\text{CO})_3]^+$  (**1**) (where R = *t*Bu or SiMe<sub>3</sub>) by displacing the  $\eta^6$ -bound *p*-xylene (Scheme 2).<sup>18</sup>



**Scheme 2:** The synthesis of an  $\eta^7$ -bound tropylium complex and the subsequent  $\eta^7,\eta^6$ -mesitylene sandwich complex.

10

From complex **1**, the carbonyl ligands could be displaced by an incoming mesitylene ligand through thermolysis in refluxing mesitylene to generate complex **2**.<sup>11</sup> Interestingly, the same reaction with toluene could not be achieved, likely as a result of its lower boiling point.

15 Complexes of the form  $[(\eta^6\text{-arene})\text{Mo}(\text{PR}_3)_3]$  are common precursors for the synthesis of heteroleptic Mo complexes and can readily be accessed by reduction of  $[\text{MoCl}_5]$  in the presence of phosphines and arene-based solvents such as toluene or 1,1-diphenylethane.<sup>19</sup>

## 2.2 Group 7: Manganese, rhenium and technetium

20 Manganese complexes of the form  $[(\eta^6\text{-arene})\text{Mn}(\text{CO})_3]^+$  can be generated from  $[\text{Mn}(\text{CO})_5]^+$ , though methods vary depending on the arene and those bearing strong electron withdrawing groups ( $-\text{CO}_2\text{H}$ ,  $-\text{NO}_2$ ,  $\text{CN}$ ) or halides are not tolerated.<sup>20</sup> As with Cr and Mo, it is possible to form  $[(\eta^6\text{-naphthalene})\text{Mn}(\text{CO})_3]^+$ , which can undergo photolytic or thermal arene exchange reactions.<sup>21</sup>

25 Although  $\text{M}(\eta^6\text{-arene})_2$  complexes are known for most transition metals, and have been extensively reviewed,<sup>22</sup> there have been relatively few examples of bis-arene complexes for the group 7 triad. Kudinov and co-workers developed a method to synthesise complexes of the form  $[\text{Re}(\eta^6\text{-arene})_2]^+$  by reduction of perrhenate salts with Zn and  $\text{AlCl}_3$  using the arene as solvent.<sup>23</sup> Direct complexation was limited to 30 hydrocarbon arenes, such as benzene, mesitylene and naphthalene. Using the latter, Alberto exploited the lability of naphthalene to generate mixed arene complexes, such as  $[(\eta^6\text{-C}_6\text{H}_6)\text{Re}(\eta^6\text{-C}_{10}\text{H}_8)]^+$ , a precursor for mono-arene complexes of the form  $[(\eta^6\text{C}_6\text{H}_6)\text{Re}(\text{L}^3)]^+$  (where L is a Lewis basic ligand).<sup>24</sup> Despite employing strong Lewis bases, displacement of benzene from the above complexes has not yet 35 been demonstrated, either thermally or photolytically, and while this stability is useful for pharmaceutical applications, they are not suitable for catalysis through arene exchange. Analogous complexes of <sup>99</sup>Tc have also been synthesised,<sup>24–26</sup> but due to their radioactivity and inherently short lifetimes, they are also unlikely to be employed as catalysts and will not be discussed further.

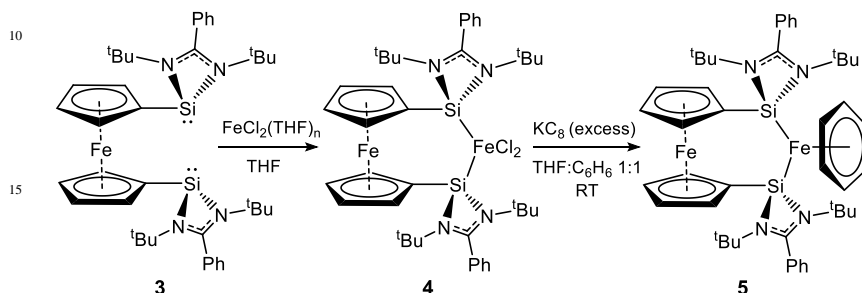
40

## 2.3 Group 8: Iron and ruthenium

Iron-based  $\pi$ -arene complexes are most commonly derived from variants of the  $\{\text{FeCp}\}^+$  fragment, however synthesis of these  $[(\eta^6\text{-arene})\text{FeCp}]^+$  complexes is challenging. Typically, ferrocene is employed as a starting material and is reacted with arenes in the presence of a strong Lewis acid, which has drawbacks when 45 employing alkyl-substituted arenes, as they can undergo a Friedel-Crafts rearrangement. Complexes with strongly electron deficient or heterocyclic arenes are also unavailable via this method. However, Kündig *et al.* reported an alternative

route to the synthesis of such complexes via  $[(\eta^6\text{-arene})\text{FeCp}]^+$  complexes with extended aromatics (e.g., pyrene), which can act as intermediates towards coordination of otherwise inaccessible arenes via arene exchange.<sup>27</sup>

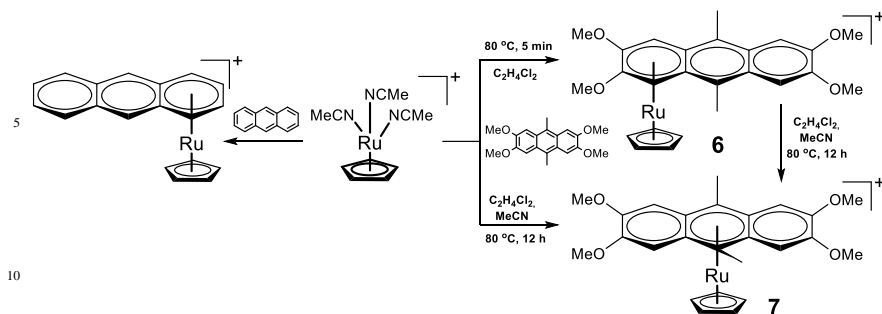
Ferrocene can often be a problematic precursor as it is extremely stable and requires harsh conditions to activate. Recently, Driess and co-workers side-stepped this issue to synthesise  $[(\eta^6\text{-arene})\text{Fe}^0\text{L}]$  complexes (**5**) (where L is a bulky, chelating 1,1'-bis(silylenyl) substituted ferrocene moiety **3**), from simple iron(II) halide salts under reducing conditions (Scheme 3).<sup>28</sup>



**Scheme 3:** Synthesis of an  $\text{Fe}^0(\eta^6\text{-benzene})$  complex from  $\text{FeCl}_2$  and a disilylferrocene ligand.

Ruthenium(II)  $\pi$ -arene complexes are typically formed by one of two methods.<sup>29</sup> The first is from the chloro-bridged dimers  $[(\eta^6\text{-arene})\text{RuCl}_2]_2$ , which can be split into monomeric species in the presence of donor ligands (L) or the Cp anion under relatively mild conditions to yield complexes of the form  $[(\eta^6\text{-arene})\text{RuL}_2\text{Cl}]^{n+}$  and  $[(\eta^6\text{-arene})\text{RuCp}]^+$ , respectively.<sup>30,31,32</sup> This approach was recently applied to the synthesis of novel  $\eta^6$ -arene ruthenium sulfide clusters of the form  $[(\eta^6\text{-C}_6\text{H}_6)_3\text{Ru}_3\text{S}_2][\text{PF}_6]_2$ , which undergoes facile, photoinduced arene dissociation in acetonitrile solutions at room temperature.

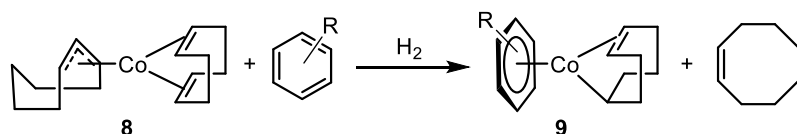
The second route to  $[(\eta^6\text{-arene})\text{RuCp}]^+$  complexes can be achieved by refluxing commercially available  $[(\text{MeCN})_3\text{RuCp}]^+$  with excess arene in weakly or non-coordinating, non-aromatic solvents (e.g., 1,2-dichloroethane). This versatile, often high yielding, approach has been used to coordinate multiple  $\{\text{CpRu}\}^+$  fragments to polyarenes<sup>33,34</sup> and is tolerant towards coordination of electron deficient arenes (e.g., benzoic acid, benzonitrile, nitrobenzene). There is still a clear preference for binding to electron rich arenes, however, and this preference is exemplified in a recent contribution from Karslyan and Perekalin.<sup>35</sup> Typically, metal fragments bind to terminal sites on anthracene, as this position is both kinetically and thermodynamically favoured (Scheme 4). However, with judicious choice of the identity and location of substituents, the authors were able to demonstrate that by shifting the majority of electron density to the central ring, it became the most thermodynamically favoured position for the Ru-arene interaction (**7**). Notably however, the terminal position remained kinetically favoured and terminally-bound Ru-anthracene conjugates (**6**) could be isolated at short reactions times. Synthesis of other Ru-arene complexes is also possible via arene exchange reactions; either photolytically<sup>36</sup> or by thermal means.<sup>37</sup>



**Scheme 4:** The binding preferences of anthracenes to ruthenium highlights the propensity towards electron rich rings and terminal rings. The conversion between the kinetic and thermodynamic products is also shown.

## 2.4 Group 9: Cobalt, rhodium and iridium

Historically,  $\pi$ -arene complexes of cobalt were derived from cobalt diene complexes such as  $[(\eta^3\text{-cyclooctenyl})\text{Co}(\eta^2,\eta^2\text{-COD})]$  (**8**, COD = cyclooctadiene) by hydrogenation of coordinated alkenes in the presence of the incoming arene and an auxiliary ligand (Scheme 5). In general, the yields of the corresponding complexes (**9**) correlated with increasing electron-density at the arene.<sup>38</sup> Further examples employed diphosphines to generate complexes of the form  $[(\eta^6\text{-arene})\text{Co}(\text{diphosphine})]^+$  from  $[(\eta^{3/5}\text{-alkenyl})\text{Co}(\text{diphosphine})]$  species.<sup>39</sup>



**Scheme 5:** Synthesis of  $\{(\eta^6\text{-arene})\text{Co}\}^+$  complexes by hydrogenation of alkenyl ligands.

Tetramethylcyclobutadienes ( $\text{Cb}^*$ ) have become popular ligands for  $\{(\eta^6\text{-arene})\text{Co}\}^+$  complexes as  $\{\text{CoCb}^*\}^+$  fragments are isolobal with  $\{\text{FeCp}^*\}^+$ , and the diene is relatively substitutionally inert.<sup>40</sup> Complexes such as  $[(\eta^6\text{-C}_6\text{H}_5\text{Me})\text{CoCb}^*][\text{PF}_6]$  (**10**) can be generated in good yields by heating  $[\text{Cb}^*\text{Co}(\text{CO})_2\text{I}]$  and an excess of  $\text{AlCl}_3$  in toluene (Figure 1A). Similar reactivity has also been reported wherein the  $\pi$ -ligands are B-substituted boroles:  $[(\eta^6\text{-arene})\text{Co}(\eta^5\text{-C}_4\text{H}_4\text{B-R})]$  (R = Cl (**11a**) or OMe (**11b**), Figure 1B).<sup>41</sup> Extending from this work, triple-decker complexes with bridging diborolyl units of the form  $[\text{CpCo}(\mu\text{-C}_3\text{B}_2\text{Me}_5)\text{M}(\eta^6\text{-arene})]$  (**12**) (where M = Rh or Ir and arene =  $\text{C}_6\text{H}_6\text{-nMe}_n$ ) have also been synthesised from the halide dimer precursors  $[\text{CpCo}(\mu\text{-C}_3\text{B}_2\text{Me}_5)\text{MBR}_2]_2$  and undergo arene exchange reactions (Figure 1C).<sup>42</sup>

For rhodium(I), common  $\pi$ -arene complexes of the form  $[(\eta^6\text{-arene})\text{Rh}(\text{PR}_3)_2]^+$  can be synthesised either from  $[\text{Rh}(\text{PR}_3)_2\text{L}]^+$  via substitution of labile ligands (L = solvent or  $\eta^2$ -olefins), or via halide abstraction from the chloro-dimers,

$[\text{Rh}(\text{PR}_3)_2]_2(\mu\text{-Cl})_2$ . The Weller group have shown arenes (most notably the non-coordinating  $[\text{B}(\text{ArF})_4]^-$  anion, where  $\text{ArF} = 3,5\text{-(CF}_3)_2\text{C}_6\text{H}_3$ ) to bind weakly to Rh(I), thereby stabilising operationally unsaturated Rh sites for catalysis.<sup>43,44</sup>

Much of the chemistry of Rh and Ir is similar to that of Co, such that many arene complexes are available from the dihalide dimers  $[\text{L}_2\text{M}]_2(\mu\text{-X})_2$  (where L is often an olefin such as ethylene,  $\eta^2$ -cyclooctene or  $\eta^2, \eta^2$ -COD) by refluxing in the arene solvent. Recent advancements show that it is possible to generate the coordinated arene *in situ* through cyclisation of alkynes and perform arene exchange experiments from these intermediates.<sup>45</sup>

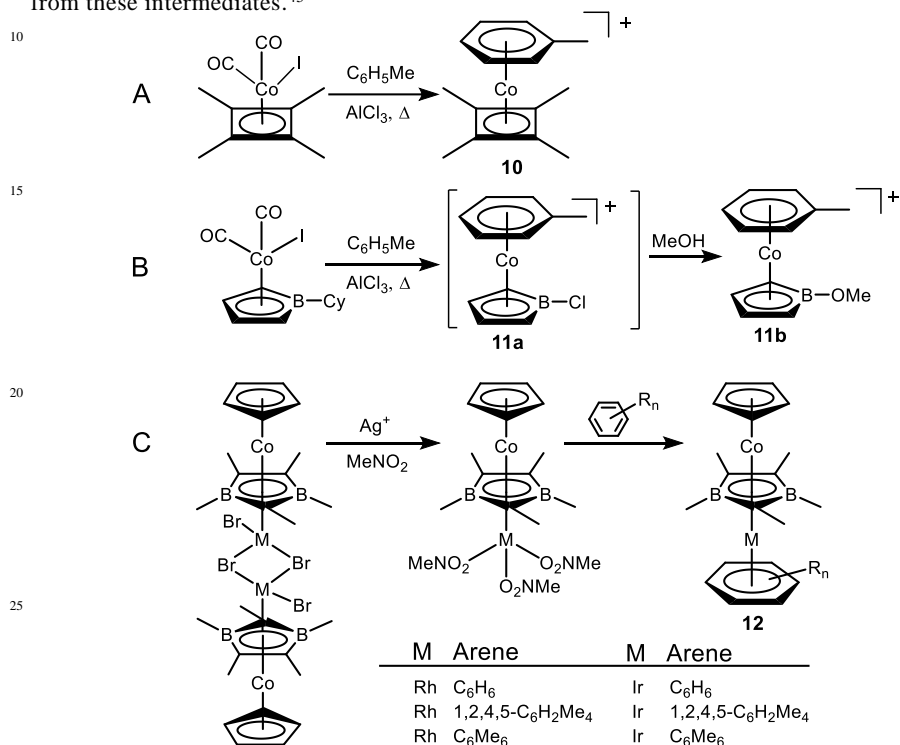


**Figure 1:** The synthesis of a family of Co sandwich complexes.

## 2.5 Group 10: Nickel, palladium and platinum

While  $\eta^6$ -arene complexes of the central transition metals are common, group 10 analogues remain far less so, with only a handful of palladium and platinum  $\eta^6$ -arene complexes reported. Perhaps one explanation for the dearth of this family comes from their thermal instability, as synthesis typically requires low temperatures (-40 °C), and long-term storage of the products at -20 °C. In most examples of  $[(\eta^6\text{-arene})\text{Ni}^0\text{L}_n]$  complexes, the arene is either toluene or benzene, but the ligands  $\text{L}_n$  can vary. In general, synthesis can be achieved by ligand substitution (or hydrogenation) of Ni olefin complexes such as  $[\text{Ni}(\text{C}_2\text{H}_4)_3]$ , or more commonly,  $[\text{Ni}(\text{COD})_2]$ , with particular success when L is a silylene<sup>46,47</sup> or an *N*-heterocyclic carbene (NHC) ligand.<sup>48</sup> In the absence of an arene solvent, it has been demonstrated that the Ni centre is able to trimerize alkynes to generate  $\eta^6$ -arene ligands *in situ*.<sup>49</sup>

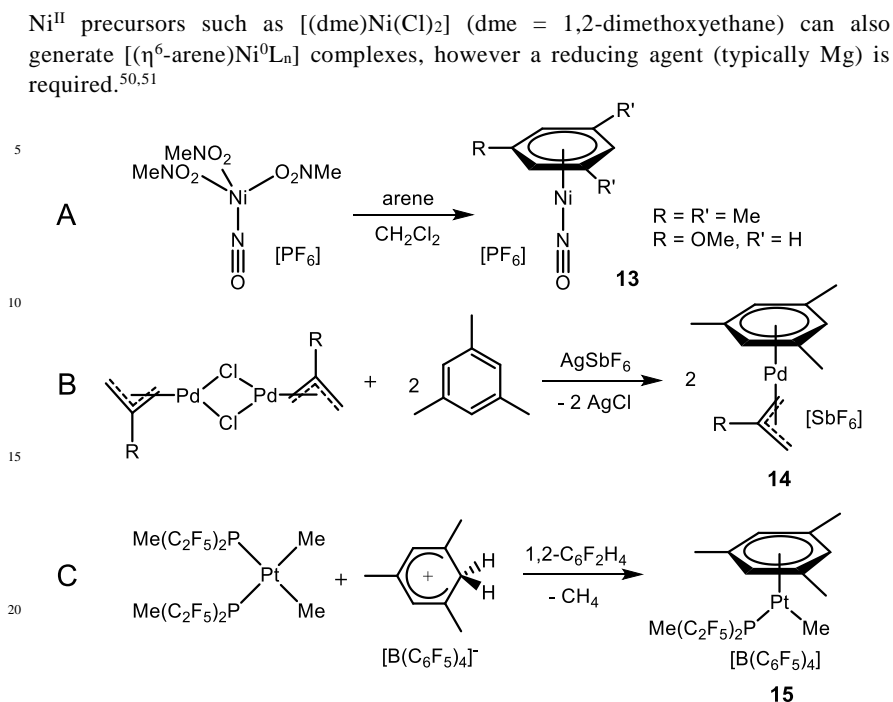


**Figure 2:** Synthetic schemes for Ni, Pd and Pt  $\pi$ -arene complexes.

An interesting example reports cationic  $\{(\eta^6\text{-arene})\text{Ni}^0\}$  complexes bearing a nitrosyl ligand (complex **13**), formed by addition of the arene to a  $\text{CH}_2\text{Cl}_2$  solution of  $[\text{Ni}(\text{NO})(\text{CH}_3\text{NO}_2)_3][\text{PF}_6]$  (Figure 2A).<sup>52</sup> In a recent advancement by Johnson and co-workers, a range of  $\{(\eta^6\text{-arene})\text{Ni}^0\}$  complexes, bearing phosphine ligands, could be synthesised and purified by the addition of *N*-methylmorpholine *N*-oxide (NMO) to arene solutions of  $[(\text{Cy}_3\text{P})_2\text{Ni}]_2\text{N}_2$  ( $\text{Cy} = \text{cyclohexane}$ ). The evolution of nitrogen from the reaction provides a convenient thermodynamic driving force, while the NMO oxidises residual phosphine, allowing facile purification by recrystallisation.<sup>53</sup>

$\{(\eta^6\text{-Arene})\text{Ni}^{\text{II}}\}$  analogues have been known for over 40 years, but remain rare.<sup>54</sup> Up until the early 2000s the major synthetic procedure was through vapour deposition of nickel metal along with the other components.<sup>55,56</sup> In 2003, however, Cámpora *et al.* used  $\text{Na}[\text{B}(\text{C}_6\text{H}_3(\text{CF}_3)_2)_4]$  to split propenyl nickel halide dimers (e.g.,  $[(\eta^3\text{-C}_3\text{H}_5)\text{Ni}]_2(\mu\text{-Cl})_2$ ) and generate isolable complexes of the form  $[(\eta^6\text{-arene})\text{Ni}^{\text{II}}(\eta^3\text{-C}_3\text{H}_5)]^+$ .<sup>57,58</sup> This approach has also been used to generate the palladium analogue  $[(\eta^6\text{-arene})\text{Pd}(\eta^3\text{-C}_3\text{H}_4\text{R})]^+$  (**14**, Figure 2B) which, to the authors knowledge, is the only example of an  $\{(\eta^6\text{-arene})\text{Pd}^{\text{II}}\}$  complex to date.<sup>59</sup> Platinum examples are almost as scarce, with only two structurally characterised examples reported.  $[(\eta^6\text{-C}_6\text{Me}_6)\text{Pt}^{\text{II}}(\eta^4\text{-C}_4\text{Me}_4)]^{2+}$  is synthesised by halide extraction of  $[(\eta^4\text{-C}_4\text{Me}_4)\text{Pt}^{\text{II}}\text{Cl}_2]$  in the presence of acetone and hexamethyl benzene,<sup>60</sup> whereas the recently reported complex  $[(\eta^6\text{-C}_6\text{H}_3\text{Me}_3)\text{Pt}(\text{PR}_3)(\text{Me})]^+$  (**15**) is formed from  $[(\text{R}_3\text{P})_2\text{Pt}(\text{Me})_2]$  and  $[\text{C}_6\text{H}_4\text{Me}_3][\text{B}(\text{C}_6\text{F}_5)_4]$  in 1,2-difluorobenzene solvent, with concomitant liberation of methane (Figure 2C).<sup>61</sup>

### 3 Ring-based reactivity of $\pi$ -arene metal complexes

As alluded to in the introduction,  $\eta^6$ -coordination of an arene to a metal alters the properties of that arene, such that reactions that were previously unfeasible become possible (Figure 3, right). The metal acts as a strong electron withdrawing group, reducing the electron density on the arene and activating many of the C-X bonds towards a broad scope of reactions, depending on the nature of X (Figure 3, left). The extent to which electron density is withdrawn depends heavily on the metal but can be equivalent to 1, 2 or even 3 nitro groups on the arene.<sup>1</sup>

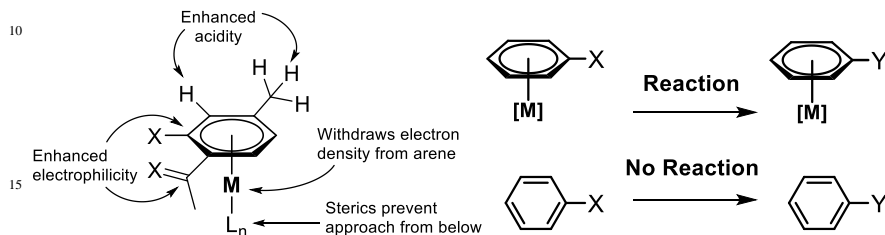


**Figure 3:** Comparing properties of free and  $\eta^6$ -bound arenes.

An additional striking effect of  $\pi$ -coordination is the increase in acidity of the C-H bonds; it is possible for the coordinated arene to deprotonate with relatively mild bases and undergo further reactions. The scope of this deprotonation chemistry has already been reviewed in the context of  $[(\eta^6\text{-arene})\text{Cr}(\text{CO})_3]$  complexes and will not be covered herein.<sup>1</sup> Furthermore, complexes such as  $[(\eta^6\text{-C}_6\text{H}_5\text{OMe})\text{Cr}(\text{CO})_3]$  are prochiral, as mono substitution in the *ortho*- or *meta*- positions generates enantiomers with planar chirality. The ramifications of this in terms of asymmetric synthesis has also been reviewed elsewhere.<sup>14,62</sup> Henceforth, this section expands on the range of reactions that open up as a consequence of arene  $\pi$ -coordination.

#### 3.1 Reactions at the ring

##### 3.1.1 C-H activation

One of the more recent and exciting developments in  $\pi$ -arene reactions is C-H activation. Typically, arene C-H bonds are relatively inert, but incorporation of an  $\eta^6$ -bound metal fragment enhances the acidity and reactivity of the C-H bonds. In a seminal paper by Fagnou *et al.*, a series of electron-poor fluoroarenes underwent direct functionalisation via a C-H concerted metalation deprotonation (CMD) mechanism.<sup>63</sup> Competition studies showed that functionalisation occurred preferentially on arenes with a greater number of fluorine substituents, highlighting the need for effective electron withdrawing groups to facilitate this chemistry. Larrosa and co-workers were the first to employ an  $\eta^6$ -bound transition metal (in this case Cr) to promote the C-H activation of otherwise unactivated arenes (i.e., those without electron-withdrawing substituents).<sup>64,65</sup> Building on Fagnou's CMD-based C-H activation, the authors were able to arylate *o*-fluorotoluene, as well as a broad scope of substituted mono-fluoroarenes (Figure 4A).

In competition experiments,  $[(\eta^6\text{-}o\text{-(F)C}_6\text{H}_4\text{Me})\text{Cr}(\text{CO})_3]$  was functionalised to give complex **16** in higher percentage conversions than both free 1,3-difluoro- and 1,3,5-trifluorobenzene but was outperformed by pentafluorobenzene. Free



2-fluorotoluene did not react at all. This clearly showcases the effect that  $\eta^6$ -coordination has on the reactivity of the arene. Using DFT it was confirmed that the role of the  $\{\text{Cr}(\text{CO})_3\}$  is both to provide an electron-withdrawing effect, increasing the acidity of the bound arene, and also to stabilise bending of the C-H bond in the transition state. Importantly, C-H activation is regioselective for the most acidic hydrogen and functionalisation occurs *ortho* to F.

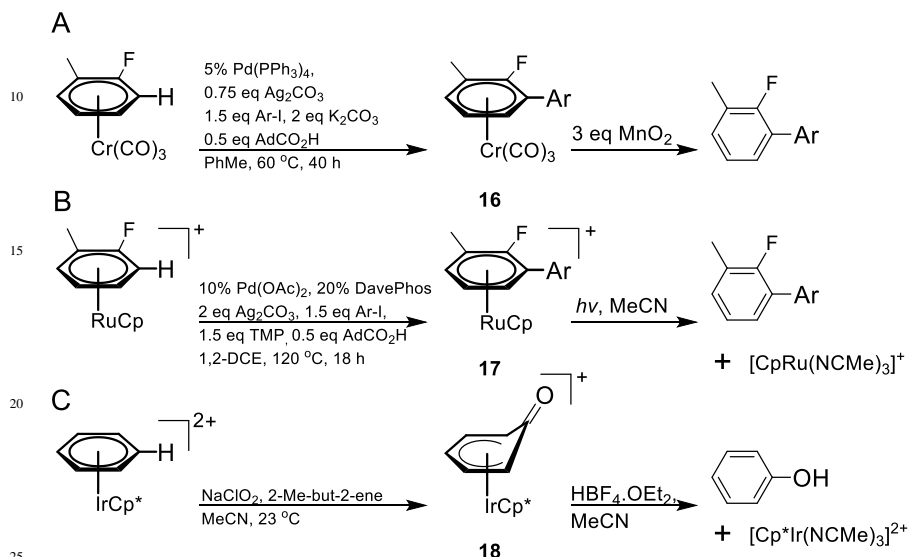


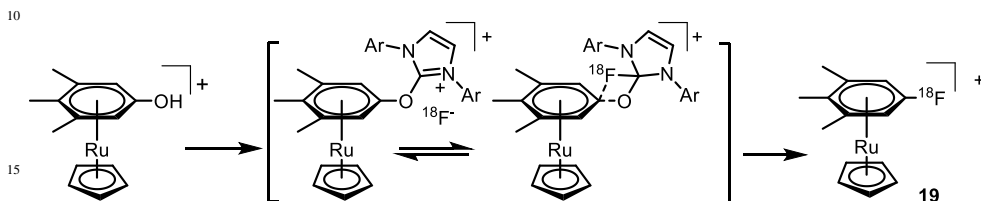
**Figure 4:** Three approaches to C-H functionalisation of  $\eta^6$ -bound arenes.

In a further development, control over regioselectivity was demonstrated to the late stage functionalisation of bioactive estradiol derivatives from *ortho*-functionalised anisoles,<sup>66</sup> using the aforementioned C-H activation approach.

These findings display a fantastic versatility and control in the C-H functionalisation of arenes, but they have one caveat: the  $(\eta^6\text{-arene})\text{-Cr}$  bond is strong and in order to liberate the newly formed biaryl, it must be oxidatively cleaved. The ability for  $[(\eta^6\text{-arene})\text{RuCp}]^+$  complexes to potentially undergo arene exchange led Walton and co-workers to explore C-H activation of  $[(\eta^6\text{-arene})\text{RuCp}]^+$  complexes (Figure 4B).<sup>67</sup> After optimisation of the C-H activation protocol, the authors showed that it was possible not only to functionalise unactivated arenes such as benzene, but also to cleave the Ru-arene bond photolytically and regenerate  $[(\text{MeCN})_3\text{RuCp}]^+$ , the reagent used to synthesise  $[(\eta^6\text{-arene})\text{RuCp}]^+$  starting complexes. This ability to recycle the  $\{\text{RuCp}\}^+$  fragment illustrates the potential for a C-H activation protocol that is catalytic in ruthenium. Similar recyclability has also been observed for a C-H hydroxylation protocol mediated by an  $\{\text{IrCp}^*\}^{2+}$  fragment.<sup>68</sup> Exploiting the enhanced electrophilicity of the  $\eta^6$ -bound arene (in this case, benzene), Ritter and co-workers employed oxygen-based nucleophiles such as  $\text{NaClO}_2$  and  $\text{H}_2\text{O}_2$  to generate  $[(\eta^5\text{-phenoxo})\text{IrCp}^*]^+$  (**18**), which could be converted to the catalytic intermediate  $[(\text{NCMe})_3\text{IrCp}^*]^{2+}$  and phenol with the addition a strong acid ( $\text{HBF}_4\cdot\text{Et}_2\text{O}$ ) in acetonitrile (Figure 4C). Unfortunately, a one-pot catalytic cycle was not possible due to the incompatibility of the strong acid and the incoming nucleophile.

### 3.1.2 Nucleophilic aromatic substitution

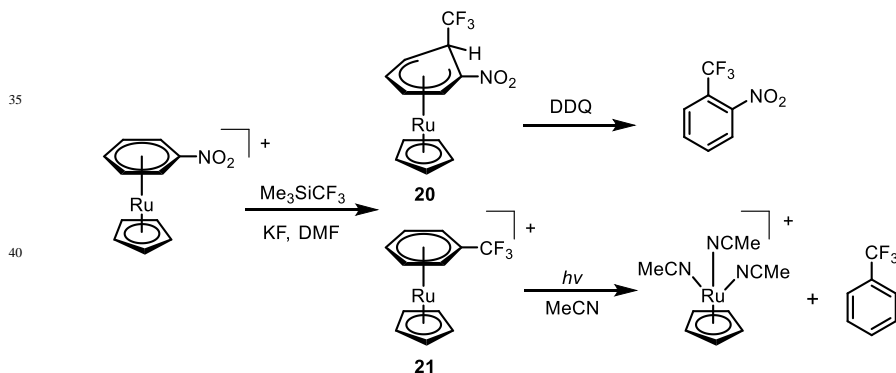
Nucleophilic aromatic substitution ( $S_NAr$ ) of arenes typically requires polarised C-X bonds and a strong electron withdrawing group (such as  $-NO_2$ ) to stabilise the negatively-charged Meisenheimer intermediate. As  $-NO_2$  functionalities are often unwanted in target reaction products, alternative approaches are desirable. Coordinating an arene to a metal centre reduces the electron density on the arene and enhances the electrophilicity of the carbon atoms in the ring, thus facilitating  $S_NAr$ .  $S_NAr$  has been undertaken successfully with metals complexes of Cr,<sup>69</sup> Mn,<sup>70</sup> Fe and Ru (e.g., in the late-stage synthesis of antibiotics).<sup>71–74</sup>



**Scheme 6:** The Pheno-Fluor-like mechanism employed in  $^{18}F$  deoxyfluorination.

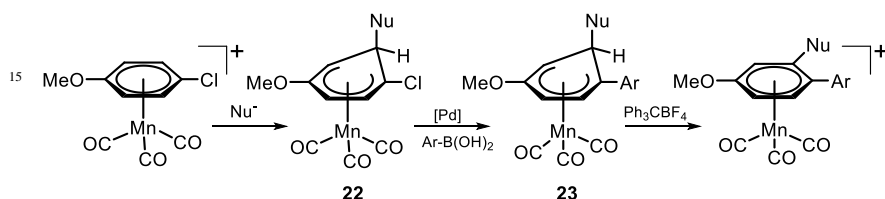
Recently, ruthenium-mediated  $S_NAr$  has been employed for radio-labelling arenes with  $^{18}F$  in a deoxyfluorination process.<sup>75</sup> Reacting  $[(\eta^6\text{-phenol})RuCp][PF_6]$  with a chloroimidazolium salt functionalises the alcohol with the imidazolium, allowing nucleophilic addition of  $^{18}F^-$  to furnish complex **19** (Scheme 6).<sup>76</sup> This process is related to the Pheno-Fluor mechanism, wherein the  $^{18}F^-$  anion is brought into proximity of the aryl-alcohol to facilitate  $S_NAr$ . Although the Pheno-Fluor process can be carried out on non-coordinated arenes with good functional group tolerance, the use of Ru increases the efficacy of this reaction and leads to fewer side products, enhancing the overall yield.

Incorporating fluorine into organic molecules is growing more and more important, with around 25% of all known pharmaceuticals or agrochemicals containing at least one F atom or  $-CF_3$  moiety.<sup>77</sup>



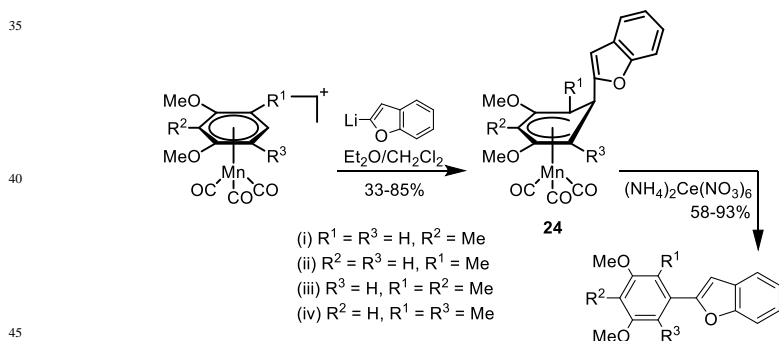
**Scheme 7:** Trifluoromethylation of  $\eta^6$ -nitroarenes and cleavage of metal-arene bond to liberate free arene.

Inspired by previous reports wherein  $C_6F_5NO_2$  was converted into  $C_6F_5CF_3$  via  $S_NAr$  with a nucleophilic source of  $CF_3$ , Walton and co-workers explored the potential to perform the related reaction on  $[(\eta^6-C_6H_5NO_2)RuCp][PF_6]$  (Scheme 7). Interestingly, two reaction products were obtained in a 1:1 ratio, namely a nucleophilic addition product  $[(\eta^5-o-(NO_2)C_6H_5CF_3)RuCp]$  (**20**) and the intended substitution product  $[(\eta^6-C_6H_5CF_3)RuCp][PF_6]$  (**21**). Variation of the reaction conditions was not able to shift the ratio of the two products. Liberation of free trifluorotoluene by photolysis led to the regeneration of  $[(MeCN)_3RuCp][PF_6]$  for use in further reactions. However, photolysis was not possible in the case of the addition product **20**, and to liberate the free arene, oxidative hydride extraction with DDQ (2,3-dichloro-5,6-dicyano-1,4-benzoquinone) was required, which also oxidised Ru to non-recovered by-products.<sup>78</sup>



**Scheme 8:** The functionalisation of Mn-bound arenes via a Meisenheimer intermediate.

The formation of Meisenheimer intermediates by nucleophilic addition to an unsubstituted position of the bond arene is not uncommon in the literature. In fact, in most electron-deficient arenes, nucleophilic addition at C-H occurs faster than at C-Cl.<sup>79</sup> Reacting  $[(\eta^6-C_6H_4(Cl)OMe)Mn(CO)_3]^+$  with nucleophiles forms the neutral Meisenheimer intermediate  $[(\eta^5-C_6H_4Nu(Cl)OMe)Mn(CO)_3]$  (**22**) which can then undergo Pd-catalysed cross-coupling reactions to furnish the ring with electron-withdrawing aryl substituents, such as aryl-aldehyde, -keto, -ester or -cyano groups (**23**). Rearomatization is achieved by reacting **23** with a hydride abstractor, such as  $Ph_3CBF_4$  (Scheme 8).<sup>80</sup> This is a particularly attractive route as it allows the formation of metal-arene complexes bearing electron withdrawing substituents that are typically unavailable via the more conventional direct complexation.

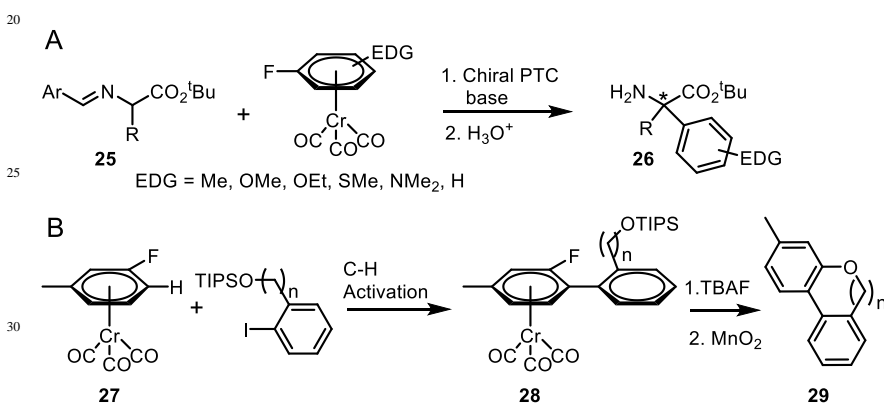


**Scheme 9:** The synthesis of stemofurans via nucleophilic addition to an  $[(\eta^6\text{arene})Mn(CO)_3]^+$  complex, followed by oxidative rearomatization.

A more recent example employed the nucleophilic substitution of hydrogen strategy (via a Meisenheimer intermediate) towards the synthesis of stemofurans (Scheme 9).<sup>81</sup> A range of  $[(\eta^6\text{-arene})\text{Mn}(\text{CO})_3]^+$  complexes (where arene = methyl/methoxy substituted benzenes) were reacted with lithiated benzofuran. Nucleophilic attack occurred at a C-H position, in preference to a C-OH or C-OMe to form the Meisenheimer intermediate **24**. The free stemofuran could be obtained through oxidative rearomatisation with  $[\text{NH}_4]_2[\text{Ce}(\text{NO}_3)_6]$ .

Another interesting example involved the addition of 2-lithio-1,3-dithiane to  $[(\eta^6\text{-C}_6\text{H}_6)\text{Mo}(\text{CO})_3]$  to generate a Meisenheimer intermediate, which was able to undergo further chemistry before arene decomplexation.<sup>82</sup> As far as the authors are aware, this example appears to be the only report of a reaction undertaken on a Mo-bound arene.

$\text{S}_{\text{N}}\text{Ar}$  has also been used to generate chiral phenylated amino esters (Figure 5A).<sup>83</sup> Reaction of an *N*-protected amino ester (**25**) with a strong base generated a nucleophilic carbon in the alpha position. In the presence of  $[(\eta^6\text{-C}_6\text{H}_5\text{F})\text{Cr}(\text{CO})_3]$  and a chiral phase-transfer catalyst, facile  $\text{S}_{\text{N}}\text{Ar}$  occurred to generate the desired phenylated *N*-protected amino esters (**26**) with excellent enantioselectivity. Addition of HCl to the reaction was sufficient to both cleave the Cr-arene bond and deprotect the amine, liberating the free phenylated amino ester **26**.

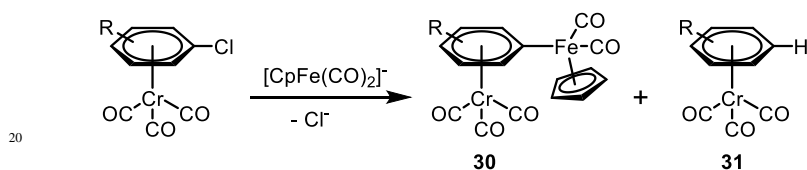


35 **Figure 5:**  $\text{S}_{\text{N}}\text{Ar}$  of  $\eta^6$ -bound arene-metal complexes. In each case, the Cr-arene bond is cleaved in the final step. PTC = phase-transfer catalyst.

Another recent example of  $\text{S}_{\text{N}}\text{Ar}$  on  $\{\text{Cr}(\text{CO})_3\}$  extends from the aforementioned C-H activation of  $[(\eta^6\text{-arene})\text{Cr}(\text{CO})_3]$  complexes (Figure 5B). Previously, excellent *ortho*-selectivity of the C-H activation of fluoro- or methoxy- benzenes had been demonstrated. Capitalising on this, the authors were able to couple 3-fluorotoluene with an aryl iodide functionalised with an alkyl chain terminated with a TIPS-protected alcohol (TIPS = triisopropylsilyl). As expected, direct arylation occurred in the 4-position (the least sterically hindered position *ortho* to F) to generate complex **28**. TIPS deprotection allowed substitution of F with the alkoxy fragment and subsequent oxidation of the  $\{\text{Cr}(\text{CO})_3\}$  fragment afforded biaryls **29**, bridged by 6, 7 and 8-membered rings. Other tethered nucleophiles such as BOC-protected amines and esters were demonstrated to undergo similar reactivity to form new C-N and C-C bonds, respectively.<sup>84</sup>

### 3.1.3 Reductive dehalogenation

In the late 1980s Heppart and co-workers were exploring the reactivities of  $[(\eta^6\text{-arene})\text{Cr}(\text{CO})_3]$  complexes with nucleophilic transition metal carbonyl species such as  $\text{K}[\text{CpFe}(\text{CO})_2]$ .<sup>85</sup> This led to the novel synthesis of a range of heterobimetallic complexes of the general form  $[(\text{L}_n\text{M}-\text{C}_6\text{H}_5)\text{Cr}(\text{CO})_3]$  (Scheme 10, complex **30**), in which the  $\eta^6$ -arene forms a direct C-M bond.<sup>86</sup> While this  $\text{S}_{\text{N}}\text{Ar}$  reactive pathway was expected, the authors observed a second pathway that was less so; namely, reductive dehalogenation to form complex **31**. In a series of investigations into the two competing pathways, a number of trends appeared. In general, electron deficient arenes tended to undergo substitution whereas those containing electron donating functionalities preferentially underwent reductive dehalogenation. However this could be overcome by introducing steric bulk at the *ortho* position; all *ortho*-disubstituted arenes investigated, including  $[(\eta^6\text{-}o\text{-C}_6\text{H}_4(\text{Cl})\text{OMe})\text{Cr}(\text{CO})_3]$  underwent reductive dehalogenation over substitution.



**Scheme 10:** Reaction of nucleophilic metal complexes with  $\eta^6$ -bound arylhalides.

The identity of the halogen was also important with  $\text{I} \gg \text{Cl} > \text{F}$  in favour of dehalogenation, and even the counteraction of the nucleophile was found to have an influence. From these trends, the authors concluded that the mechanism of reductive dehalogenation likely occurs via a SET (single electron transfer) mechanism followed by hydrogen atom extraction from the solvent. Recent studies have shown that excluding available hydrogen atoms can favour the substitution pathway. In a THF solution of  $[(\eta^6\text{-C}_6\text{H}_5\text{I})\text{Cr}(\text{CO})_3]$  and nucleophilic  $\text{K}[\text{Cp}^*\text{Fe}(\text{CO})_2]$ ,  $\text{S}_{\text{N}}\text{Ar}$  was observed, whereas addition of *t*BuOH to the reaction leads exclusively to the dehalogenation complex  $[(\eta^6\text{-C}_6\text{H}_6)\text{Cr}(\text{CO})_3]$ .<sup>87</sup> This has potential to be an important reaction, as it provides a pathway for the safe disposal of polychloro-aromatic hydrocarbons, potential environmental pollutants.<sup>88</sup>

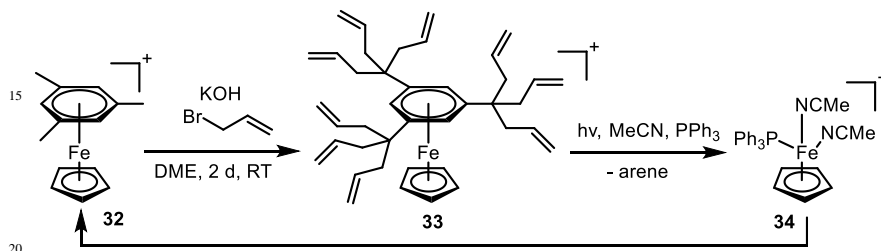
## 3.2 Reactions at sites beyond those directly coordinated

### 3.2.1 Deprotonation and ester formation/hydrolysis

Important properties of  $\text{M}(\eta^6\text{-arene})$  complexes are the enhanced acidity and electrophilicity of the aromatic ring. We have already discussed the advantages that this provides in the context of C-H activation and nucleophilic addition, but these properties have been shown to extend beyond the directly-coordinated ring, such that aromatic alcohols and benzylic protons can be deprotonated with ease.

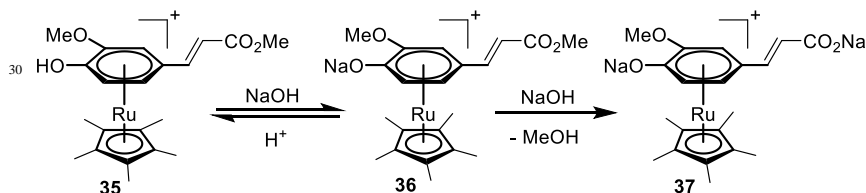
DuBois and co-workers reported that when  $[(\eta^6\text{-}p\text{-cymene})\text{Ru}(\text{H-indole})]^{2+}$  was eluted through an alumina column, the compound that resulted was the *N*-deprotonated complex,  $[(\eta^6\text{-}p\text{-cymene})\text{Ru}(\text{indole})]^+$ .<sup>89</sup> This result could be reproduced and conveniently reversed in solution by washing with aqueous NaOH and triflic acid solutions, respectively. Indeed, subsequent reports have found that the  $\text{pK}_a$  of the NH indole proton in  $\eta^6$ -bound tryptophan complexes is around 8

orders of magnitude lower than free indole. Similarly, the  $pK_a$  of the phenolic protons of L-DOPA (L-3,4-dihydroxyphenylalanine) decrease from 9.83 to 3.67 when L-DOPA is  $\eta^6$ -bound to Ru.<sup>90</sup> This ease of deprotonation has been exploited to tremendous effect by Astruc and co-workers, as a method for synthesising effective  
 5 nuclei for dendrimers (Scheme 11).<sup>91,92</sup> By reacting  $[(\eta^6\text{-C}_6\text{H}_3\text{Me}_3)\text{FeCp}][\text{PF}_6]$  (**32**) and allylbromide with KOH in DME (dimethoxymethane), it is possible to completely deprotonate and functionalise each of the nine benzylic protons in the complex to form **33** in just two days at room temperature. Once the reaction is complete, the iron-arene bond can be cleaved by photolysis and the iron-catalyst  
 10 (**34**) regenerated. However, as yet, there is no report of a one-pot system that is catalytic in iron.



**Scheme 11:** The nona-allylation of  $\eta^6$ -bound mesitylene for the synthesis of dendritic cores.

The facile deprotonation of  $\eta^6$ -bound lignol complexes of Mn and Ru has also been  
 25 demonstrated.<sup>93</sup> In the context of breaking down lignin, both Ru and Mn have been shown to coordinate in an  $\eta^6$  fashion to the aromatic moieties in lignin, although the Ru complexes (**35**) were found to be more stable.



**Scheme 12:** Facile phenolic deprotonation, followed by remote ester hydrolysis, facilitated by an  $\eta^6$ -bound  $\{\text{RuCp}^*\}^+$  fragment.

As illustrated in Scheme 12, deprotonation of phenolic moieties occurs readily in aqueous NaOH to form complex **36**, but gratifyingly, a second equivalent of NaOH  
 40 is able to hydrolyse a remote ester functionality, generating **37**. This process indicates the potential of these organometallic reagents to separate lignin from cellulose in biomass. Furthermore, hydrolysis was found to occur at a rate around 100 times faster than in the free un-coordinated lignol, highlighting the profound effects that the electron-withdrawing  $\{\text{RuCp}^*\}^+$  unit has on remote functionalities.  
 45 This enhanced reactivity of ester functionalities was further probed for the synthesis of new cytotoxic organometallics.<sup>94</sup> Starting from  $[(\eta^6\text{-C}_6\text{H}_5\text{CO}_2\text{Me})\text{RuCp}^*][\text{BF}_4]$ , ester hydrolysis was achieved with NaOH in aqueous MeOH within 30 minutes to generate the corresponding carboxylic acid upon acid workup. The enhanced electrophilic nature of the carboxylic acid allowed the synthesis of a range of esters

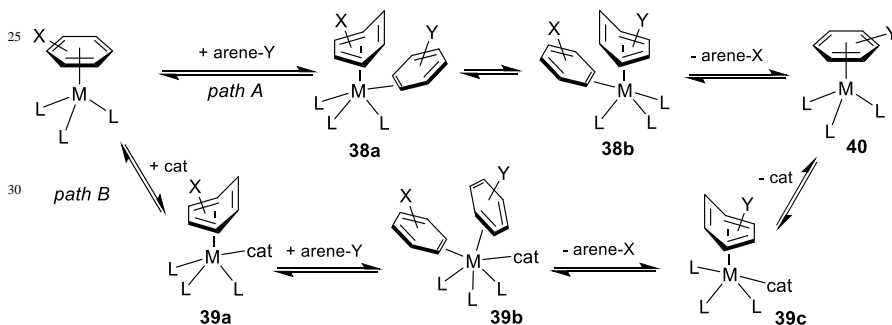
and amides from  $[(\eta^6\text{-C}_6\text{H}_5\text{CO}_2\text{H})\text{RuCp}^*]$  under a variety of substitution conditions using alcohols and primary/secondary amines, respectively. Subsequent *in vitro* studies illustrated the ability of the  $[(\eta^6\text{-arylester})\text{RuCp}^*]^+$  complexes to inhibit growth in several tumourigenic cell lines in low micromolar concentrations.

## 5 4 Arene exchange in $\pi$ -arene metal complexes

As shown in the previous chapter, there is a wide range of novel reactions of aromatic compounds that are only feasible when the arene is  $\pi$ -coordinated to a metal centre. While several methods are known to allow decomplexation of the  $\pi$ -coordinated product after the reaction is complete, a more desirable situation is to achieve catalytic turnover under the reaction conditions. In an ideal scenario, an arene would  $\pi$ -coordinate to a metal centre, react and then exchange for a second equivalent of arene starting material. To achieve this catalytic process, arene exchange must be feasible under the reaction conditions. To develop such a reaction, a detailed understanding of the mechanism of arene exchange and the factors that affect the rate and extent of this process is required. In this section, we summarise the fundamental understanding of arene exchange, with a view to application in catalytic reactions.

### 4.1 Mechanism of arene exchange

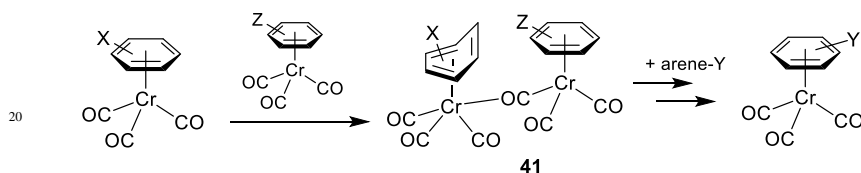
The mechanism of thermal arene exchange has been of interest for several decades, with several theories proposed.<sup>95</sup> The currently accepted mechanism of arene exchange is shown in Scheme 13.<sup>96,97</sup> This mechanism has been established for  $[(\eta^6\text{-arene})\text{Cr}(\text{CO})_3]$  complexes,<sup>98</sup> but similar mechanisms have been proposed for other metal ligand combinations (*vide infra*).



35 **Scheme 13:** Mechanism of arene exchange. cat = catalysing ligand (e.g. solvent).

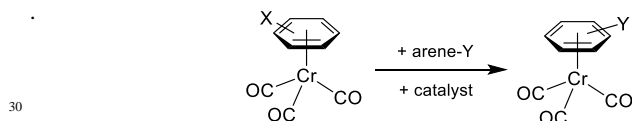
Two potential mechanistic routes are shown depending on whether the exchange is uncatalysed (*path A*) or catalysed (*path B*) by a coordinating ligand. In the first step of each pathway, the coordinated arene goes from  $\eta^6$ -coordination to  $\eta^4$ -coordination. The first intermediate (**38a** or **39a**) contains an additional ligand in the exposed position. In *path A* this ligand is the incoming arene, while in *path B* this is a catalysing ligand. This initial step is dissociative in the transition state and is the rate limiting step of arene exchange. The next step for *path B* involves the coordination of the incoming arene to give **39b**. From intermediates **38a** and **39b**, an un-zipping and zipping process completes the arene exchange mechanism. The choice of *path A* or *path B* depends upon the reaction conditions. In neat incoming

arene or in non-coordinating solvents (cyclohexane, di-*n*-butyl ether), *path A* is followed, giving a rate of reaction dependent upon both initial complex and incoming arene. When a coordinating solvent (THF, cyclohexanone, acetone) is employed, *path B* is followed with the solvent acting as the catalysing ligand. Under these conditions, the rate of exchange becomes independent of the incoming arene.<sup>99</sup> This can also be the case with even a small amount of catalytic coordinating solvent in bulk non-coordinating solvent is used. In the specific case of arene exchange in  $[(\eta^6\text{-arene})\text{Cr}(\text{CO})_3]$  complexes, *path B* can proceed with the initial mechanistic step catalysed by a second metal-arene complex.<sup>100</sup> This can be the starting complex or an added catalytic complex, such as  $[(\eta^6\text{-C}_6\text{Me}_6)\text{Cr}(\text{CO})_3]$ . In this case, catalysis has been suggested to proceed via intermediate **41**, in which the carbonyl ligand oxygen of one complex coordinates to the second complex during the rate-limiting  $\eta^6 \rightarrow \eta^4$  step (Scheme 14). An approximate comparison of rates depending upon choice of catalyst is given in Table 1.<sup>97</sup> The comparison illustrates the large influence of coordinating ligands in the arene exchange process.



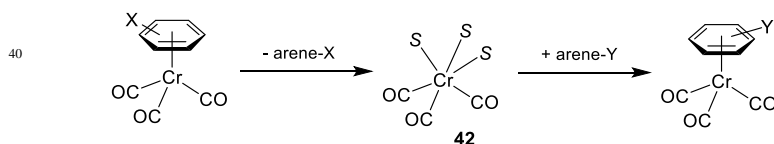
**Scheme 14:** Arene exchange catalysed by a second  $[(\eta^6\text{-arene})\text{Cr}(\text{CO})_3]$  complex.

**Table 1:** Rate enhancement by selected catalysing solvents or Cr complex (adapted from reference 97).



Catalyst	$k_{\text{catalysed}}/k_{\text{uncatalysed}}$ ( $\text{M}^{-1}$ )	Catalyst	$k_{\text{catalysed}}/k_{\text{uncatalysed}}$ ( $\text{M}^{-1}$ )
Cyclohexanone	1300	Diglyme	200
PhCN	600	THF	30
Cyclooctadiene	200	$[(\eta^6\text{-C}_6\text{Me}_6)\text{Cr}(\text{CO})_3]$	30

In each of the un-zipping and zipping steps, coordinating solvents may also play a role through transient coordination. An alternative mechanism has also been suggested in which the initial arene fully dissociates to form  $[(S)_3\text{Cr}(\text{CO})_3]$  (**42**, *S* = solvent) before the second arene coordinates (Scheme 15).<sup>97</sup> This is particularly likely in strongly coordinating solvents and with weakly coordinated arenes.



**Scheme 15:** Arene exchange via solvated intermediate **42** (*S* = solvent).



## 4.2 Dependence on incoming and outgoing arene

The rate and extent of arene exchange will depend upon the outgoing arene and, in uncatalysed reactions, on the incoming arene. Thermodynamic stabilities of  $[(\eta^6\text{-arene})\text{Cr}(\text{CO})_3]$  complexes follow the electronic properties of the arene, with electron rich arenes binding more strongly than electron poor arenes (Figure 6).<sup>98</sup> The rate of arene exchange has been shown to somewhat mirror the order of thermodynamic stabilities, with electron-rich  $[(\eta^6\text{-C}_6\text{Me}_6)\text{Cr}(\text{CO})_3]$  slowest to exchange and electron-poor  $[(\eta^6\text{-}p\text{-C}_6\text{H}_4\text{F}_2)\text{Cr}(\text{CO})_3]$  fastest.<sup>98,101</sup>

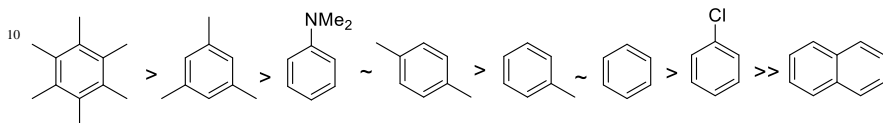
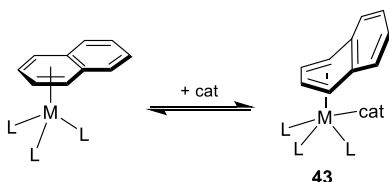


**Figure 6:** Order of stability in  $[(\eta^6\text{-arene})\text{Cr}(\text{CO})_3]$  complexes.<sup>98</sup>

15

In complexes of the form  $[(\eta^6\text{-arene})\text{RuCp}]^+$ , the arene is particularly labile when the capping arene is naphthalene<sup>102</sup> or other polyaromatics.<sup>103,104</sup> This is due to partial retention of aromaticity in the  $\eta^4$ -bound intermediate (**43** in Scheme 16). By contrast, bound six-membered rings lose aromaticity upon haptotropic shift to  $\eta^4$  binding, resulting in much slower thermal arene displacement in complexes such as  $[(\eta^6\text{-C}_6\text{H}_6)\text{RuCp}]^+$ . The lability of the arene in  $[(\eta^6\text{-naphthalene})\text{RuCp}]^+$  provides a useful synthetic route to novel  $[(\eta^6\text{-arene})\text{RuCp}]^+$  complexes. Kudinov and Perekalin<sup>105</sup> and others<sup>106,107</sup> have exploited this chemistry particularly well. In arene exchange reactions involving incoming arenes with multiple potential aromatic binding groups, coordination to the least sterically hindered ring is the kinetic product from where haptotropic rearrangements can take place to the thermodynamically more stable complex, with the more electron-rich ring bound to Ru.<sup>108,109</sup> Related intramolecular arene exchange has also been observed in Rh(I) complexes.<sup>110</sup>

30



35

**Scheme 16:** Initial haptotropic shift in  $\pi$ -coordinated naphthalene–metal complexes.

## 4.3 Dependence on metal and ligands

While much of the mechanistic evidence for arene exchange comes from the study of  $[(\eta^6\text{-arene})\text{Cr}(\text{CO})_3]$  complexes, arene exchange is also observed in many other complexes. The rate of exchange will naturally depend upon the choice of metal and ligand. For example, complex **44**, containing Ru(II) and a strongly electron-donating silyl xantsil ligand, will undergo arene exchange in benzene at room temperature in one hour (Figure 7A).<sup>111</sup> The added electron density at the Ru centre reduces the stability of the  $\eta^6$ -coordinated electron-rich aromatic ligand. Silyl ligands have also produced complexes displaying room temperature arene exchange in Fe(0) complexes<sup>112</sup> and in Ni(0) complexes<sup>113</sup> (Figure 7B and 7C). While arene exchange in Ni(II) complexes has been known for many years,<sup>114</sup> the ability to synthesise stable  $\{(\eta^6\text{-arene})\text{M}\}$  complexes of Ni(0) (which is itself electron-rich) is allowed by

the use of ylide-like silylene ligands, which are  $\pi$ -accepting, giving fast arene exchange in complexes such as **46**. Alternative ligands for Ni(0) stabilisation are NHC ligands, which can also accept  $\pi$ -electron density from the Ni(0) centre to allow the synthesis of stable  $[(\eta^6\text{-arene})\text{Ni}^0\text{L}]$  complexes, which undergo arene exchange at room temperature in 5 mins.<sup>48</sup>

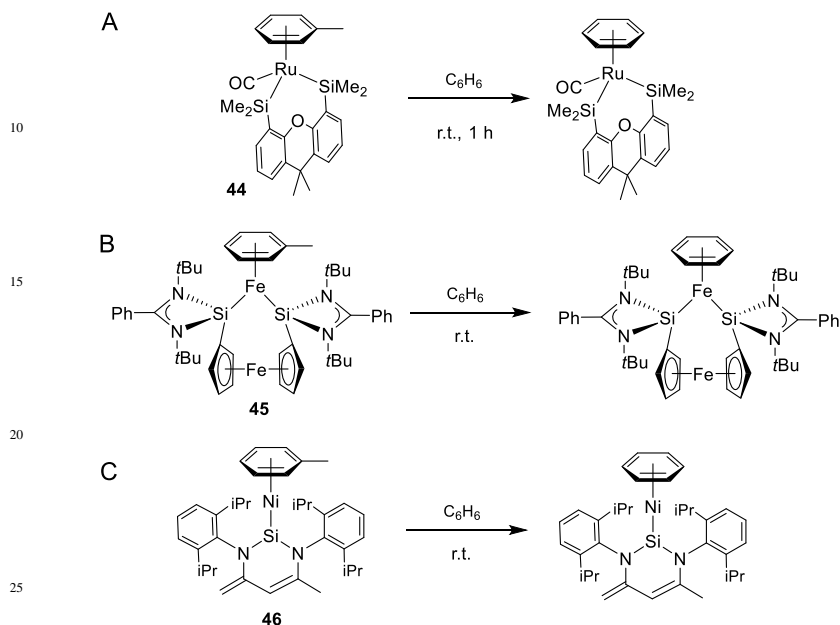


**Figure 7:** Examples of complexes with strongly electron-donating ligands displaying room temperature arene exchange.

Another class of metal-arene complexes that can undergo room temperature arene exchange is the  $[(\eta^6\text{-arene})\text{Mo}(\text{CO})_3]$  complexes. Thermodynamic bond enthalpies for M-arene in  $[(\eta^6\text{-arene})\text{Cr}(\text{CO})_3]$  and  $[(\eta^6\text{-arene})\text{Mo}(\text{CO})_3]$  are 53 kcal mol<sup>-1</sup> and 68 kcal mol<sup>-1</sup>, respectively.<sup>115</sup> However, the lability of the bound arene does not follow the thermodynamic stability, with  $[(\eta^6\text{-arene})\text{Mo}(\text{CO})_3]$  undergoing arene exchange at room temperature in THF (Figure 8A).<sup>12</sup> Kündig showed that incoming electron-rich arenes could replace  $\eta^6$ -bound benzene in several hours at room temperature, while electron-poor incoming arenes were not isolated due to the apparent instability of the resultant complexes.<sup>12</sup> More recently, Bradley has shown that the rate of arene exchange in  $[(\eta^6\text{-arene})\text{Mo}(\text{CO})_3]$  is dependent upon the sterics of the coordinated arene (Figure 8B and 8C).<sup>116</sup> Complex **48**, with a moderately large  $\eta^6$ -coordinated arene, required heating at 70 °C in neat C<sub>6</sub>D<sub>6</sub> to allow arene exchange, while complex **49**, incorporating a more sterically hindered arene showed no exchange at all in neat C<sub>6</sub>D<sub>6</sub>. When THF - with the capability to catalyse arene exchange - was employed as the solvent, complex decomposition occurred. DFT studies confirmed that kinetics dictate the arene exchange process, as the more bulky arenes in this study were also found to be the least thermodynamically stable. Beyond those mentioned here, other examples of metal complexes displaying room temperature arene exchange include Pt(II) electron-deficient phosphine complexes,<sup>117</sup> Pd(II) allyl complexes<sup>118</sup> and Sc  $\beta$ -diketiminato complexes.<sup>119</sup>

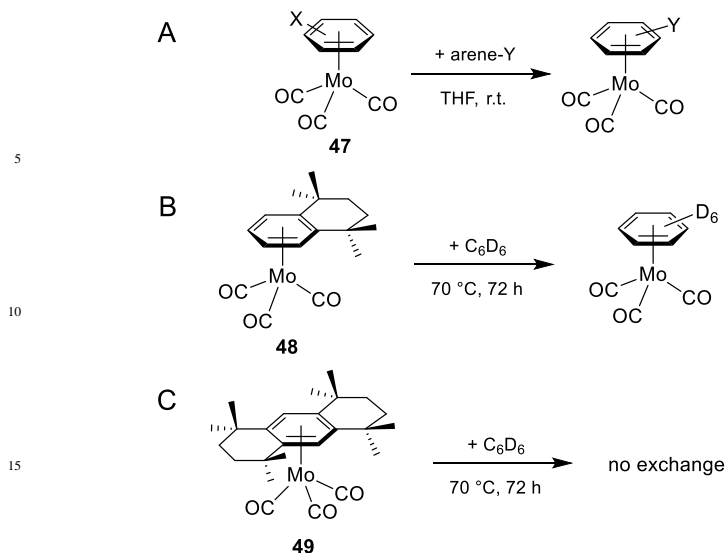


**Figure 8:** Examples of arene exchange in Mo complexes.

#### 20 4.4 Accelerating Arene Exchange with Tether Complexes

As shown above, the rate of arene exchange can be enhanced by incorporating catalysing ligands that coordinate to the metal centre during the  $\eta^6$  to  $\eta^4$  haptotropic shift. An alternative approach uses intramolecular tethers built into the metal complex that can coordinate to the metal centre during this initial rate limiting step.

25 The first example of such a system involved replacement of one of the CO ligands in  $[(\eta^6\text{-C}_6\text{H}_6)\text{Cr}(\text{CO})_3]$  with a methylacrylate ligand to give complex **50a** (Figure 9A).<sup>120</sup> During the rate-limiting  $\eta^6$  to  $\eta^4$  step of arene exchange the carbonyl of the methylacrylate can coordinate to Cr to give intermediate **50b**. The ability of methylacrylate to undergo a change in hapticity allows arene exchange to proceed at

30 room temperature for a range of incoming arenes. Note that the analogous reaction for  $[(\eta^6\text{-arene})\text{Cr}(\text{CO})_3]$  requires heating to 170 °C.<sup>97</sup> Using a similar strategy, Semmelhack showed efficient arene exchange in Cr complexes with tris(pyrrole)phosphine ligands, incorporating an additional tether group capable of coordinating to the Cr centre (Figure 9B).<sup>121</sup> In this detailed study, a clear

35 correlation was established between the donating ability of the tether and the rate of arene exchange (Table 2). In further kinetic analysis on the arene exchange of **51a** (L = CO<sub>2</sub>Me), transition state data for  $\Delta H^\ddagger$  and  $\Delta S^\ddagger$  were calculated as 22 kcal mol<sup>-1</sup> and -2.8 cal mol<sup>-1</sup> K<sup>-1</sup>, respectively, giving evidence for a dissociative transition state. It is also important to note that the rate equation in this series can depend both

40 on the incoming and outgoing arene. This highlights that the reaction kinetics is highly dependent upon the system under study and that a ‘one-size-fits-all’ mechanistic description, such as that given in Scheme 13, must be used with caution.

Tether complexes have also been shown to accelerate arene exchange in Ru complexes. Walton reported several  $[(\eta^6\text{-}p\text{-cymene})\text{Ru}(\text{CpR})]^+$  tether complexes

45 (where CpR is a cyclopentadienyl ligand with a tether ligand incorporated) that showed accelerated arene exchange, compared to the parent complex  $[(\eta^6\text{-}p\text{-cymene})\text{RuCp}]^+$  (Figure 9C).<sup>32</sup> Again, a correlation was observed between the donating ability of the tether ligand and the rate of arene exchange, with the pyridyl

tether complex **52a** showing an 18-fold increase in arene exchange rate compared to the parent complex. In related work, Wills has also shown the use of coordinating tethers to synthesise Ru–arene transfer hydrogenation catalysts.<sup>122</sup> An  $[(\eta^6\text{-C}_6\text{H}_5(\text{CO}_2\text{Et}))\text{RuCl}_2]_2$  dimer is reacted with a TsDPEN-derived arene. Initial coordination of one amine group of TsDPEN brings the arene close to the Ru centre, facilitating arene exchange with the  $\eta^6$ -bound arene producing the desired Ru(II) transfer hydrogenation catalyst.

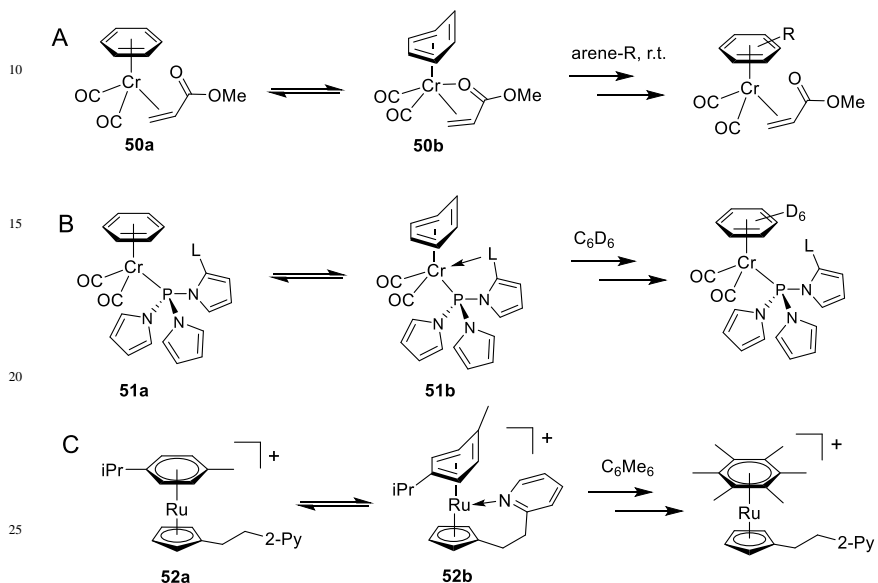
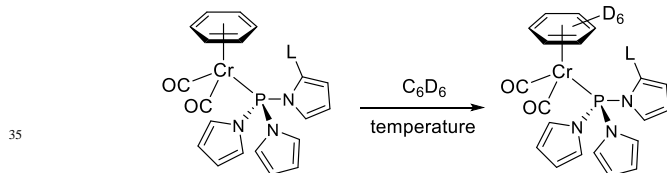


**Figure 9:** Complexes incorporating tethers that catalyse arene exchange.

**Table 2:** Rate of arene exchange as a function of tether donating ability.<sup>121</sup>



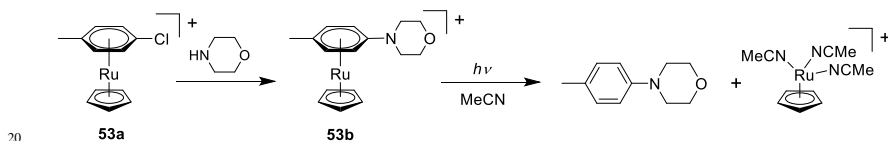
Pyrrole substituent, L	Temp / °C	Exchange Half-life	Pyrrole substituent, L	Temp / °C	Exchange Half-life
–CO <sub>2</sub> Me	70	0.5 h	–CO <sub>2</sub> Me	23	115 h
–SMe	70	8.7 h	–CONMe <sub>2</sub>	22	9 h
–SPh	70	30.6 h	–2-Py	22	8 h
–SF <sub>3</sub>	70	>150 h			

#### 4.5 Photocatalytic arene exchange

As an alternative to thermal activation, photolysis has been routinely used to liberate  $\eta^6$ -bound arenes from metal complexes. Typically, photolysis leads to release of the free arene and the newly-available coordination sites on the metal complex are

occupied by solvent molecules. The ability to achieve photocatalytic arene exchange, however, has been somewhat less well explored. In this section, we summarise the accepted mechanisms of photocatalytic arene exchange and discuss several examples of exchange in metal-arene complexes.

Perhaps the most prolific use of photolysis of metal-arene species is with  $[(\eta^6\text{-arene})\text{FeCp}]^+$  and  $[(\eta^6\text{-arene})\text{RuCp}]^+$  complexes.<sup>123,124</sup> One early example reported by Woodgate shows a  $\text{S}_{\text{N}}\text{Ar}$  between  $\eta^6$ -coordinated chlorobenzene (**53a**) and morpholine, followed by photolysis of the  $\eta^6$ -bound product (**53b**) with UV irradiation (Rayonet photoreactor at 300 nm) in acetonitrile, which generates  $[(\text{MeCN})_3\text{RuCp}]^+$  as the only by-product (Scheme 17).<sup>125</sup> In the specific case of photolysis of  $[(\eta^6\text{-arene})\text{RuCp}]^+$  in MeCN, the quantum yield for arene loss follows the order: benzene > toluene > mesitylene >  $\text{C}_6\text{Me}_6$ .<sup>126</sup> This order reflects both the electronic factors, due to a slight build-up of negative charge at the arene in the transition state (*vide infra*) and steric factors, as more bulky arenes render the metal centre less accessible to incoming solvent.



**Scheme 17:** Photolysis used to liberate the product of  $\text{S}_{\text{N}}\text{Ar}$ .<sup>125</sup>

At low temperatures ( $-40\text{ }^\circ\text{C}$ ), the analogous complex  $[(\eta^6\text{-arene})\text{FeCp}]^+$  undergoes photolysis (either sunlight or 100 W mercury lamp) in acetonitrile to give  $[(\text{MeCN})_3\text{FeCp}]^+$  (Figure 10A).<sup>127</sup> This species is unstable with respect to solvolysis and ligand rearrangement to give  $[\text{Fe}(\text{NCMe})_6]^{2+}$  and ferrocene at room temperature. In non-coordinating solvents (e.g.,  $\text{CH}_2\text{Cl}_2$ ), photocatalytic arene exchange is feasible for  $[(\eta^6\text{-arene})\text{FeCp}]^+$  if the incoming arene is more electron-rich than the outgoing arene.<sup>128</sup> Bright sunlight was enough to allow for arene exchange between  $[(\eta^6\text{-}p\text{-xylene})\text{FeCp}]^+$  (**54**) and  $\text{C}_6\text{Me}_6$  within 5 hours (Figure 10B). The analogous reaction with  $[(\eta^6\text{-}p\text{-xylene})\text{RuCp}]^+$  (**55**) does not take place.

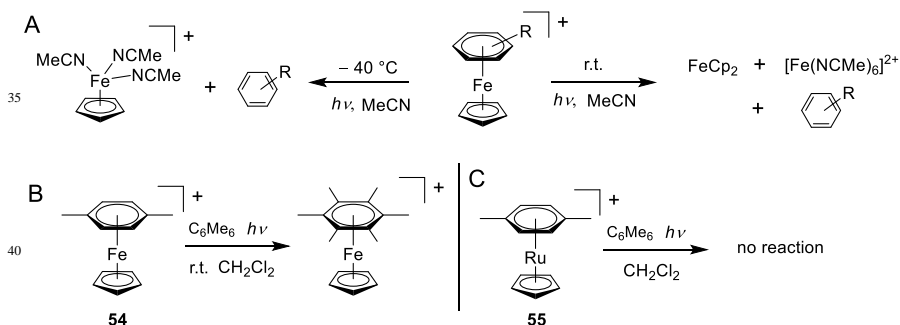


**Figure 10:** Photocatalytic processes of Fe and Ru  $\pi$ -arene complexes.

Photocatalytic arene exchange is not observed for  $[(\eta^6\text{-C}_6\text{H}_6)\text{RuCp}]^+$ , but has recently been shown to be feasible for complexes in which the initial  $\eta^6$ -bound species is polyaromatic. Exchange was measured for  $[(\eta^6\text{-DBT})\text{RuCp}]^+$  (**56**, DBT = dibenzothiophene) in the presence of 1 equivalent of incoming arene in acetone

under UV irradiation (450 W low-pressure immersion lamp) at 25 °C (Figure 11A).<sup>129</sup> The reported equilibrium constant ( $K_{\text{eq}} = [\{(\eta^6\text{-arene-R})\text{RuCp}\}^+] / [\{(\eta^6\text{-DBT})\text{RuCp}\}^+]$ ) for various incoming arenes followed the order: mesitylene (17) > toluene (13) > benzene (5.9) > naphthalene (0.35). The extent to which this process is in equilibrium was not discussed in the report and it may be that the values are more a measure of conversion rather than equilibrium values. Note that the order of preference for incoming arene mirrors the thermally promoted reaction in  $[(\eta^6\text{-C}_6\text{H}_6)\text{Cr}(\text{CO})_3]$  ( $M = \text{Cr}, \text{Mo}$ ).

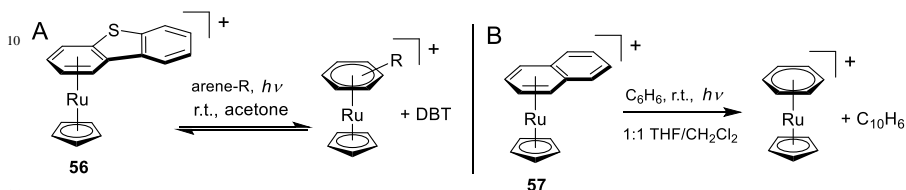


**Figure 11:** Photocatalytic arene exchange of Ru-polyaromatic complexes.

$[(\eta^6\text{-Naphthalene})\text{RuCp}]^+$  (**57**) will also undergo photocatalytic arene exchange (Figure 11B).<sup>130</sup> In the presence of 3 equivalents of benzene in  $\text{CH}_2\text{Cl}_2$  arene exchange of **57** ( $[\text{PF}_6]^-$  salt) proceeded to 10% conversion after 6 h (650 W mercury lamp). The conversion could be increased to 33% by the addition of the weakly-coordinating anion  $[\text{CF}_3\text{SO}_3]^-$  and complete arene exchange was achieved in 12 hours when coordinating co-solvents (e.g. THF) were employed. Interestingly, when the incoming arene was changed to  $\text{C}_6\text{Me}_6$  arene exchange conversion was low: 10% under the same conditions, highlighting the kinetic barrier of incoming bulky arenes. The preference for incoming arene follows the order: *p*-xylene > benzene >  $\text{C}_6\text{Me}_6$ . This illustrates the balance between sterics and electronics in the photocatalysed arene exchange process.

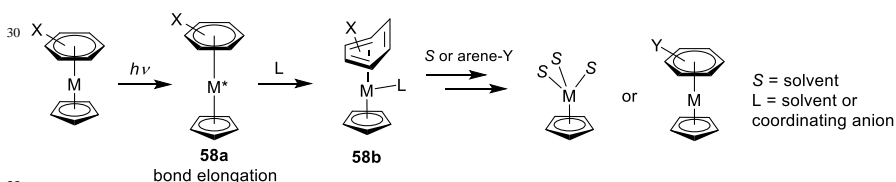


**Figure 12:** Mechanism of photocatalytic arene exchange in  $[(\eta^6\text{-arene})\text{MCp}]^+$  ( $M = \text{Fe}, \text{Ru}$ ).

The mechanism of photolysis of  $[(\eta^6\text{-arene})\text{MCp}]^+$  ( $M = \text{Fe}, \text{Ru}$ ) is proposed to proceed via a metal-centred photoexcited state that promotes an electron from a metal-centred  $d(z^2)$  orbital to a metal-centred  $d(xz)$  or  $d(yz)$  (Figure 12).<sup>131</sup> The initial singlet state rapidly intersystem crosses to the triplet state. Population of the  $d(xz)/d(yz)$  orbitals leads to elongation of the metal–arene bond and build-up of negative charge at the arene (**58a**). Depopulation of the  $d(z^2)$  orbital allows for nucleophilic attack at the metal centre in the excited state, giving a likely  $\eta^4$ -coordinated intermediate (**58b**) from where arene exchange (for solvent or an incoming arene can take place). Such nucleophilic attack may be from nucleophilic solvents, such as MeCN, but can also be from the counterion of the cationic complex. It is observed that in non-coordinating  $\text{CH}_2\text{Cl}_2$ , the quantum yield for

photocatalytic conversion of  $[(\eta^6\text{-}p\text{-xylene})\text{FeCp}]\text{X}$  to  $[\text{Fe}(\text{phen})_3]^{2+}$  (phen = phenanthroline) depends upon the counterion, X, and follows the order  $[\text{BF}_4]^- > \text{Br}^- \gg [\text{PF}_6]^- > [\text{SbF}_6]^-$ .<sup>132</sup> The analogous photolysis of  $[(\eta^6\text{-C}_6\text{H}_6)\text{OsCp}]\text{X}$  in acetonitrile does not take place when  $\text{X} = [\text{PF}_6]^-$ , but is complete within 3 hours for the  $\text{X} = \text{Br}^-$  complex.<sup>133</sup> This highlights the potential importance of ion-pairs in the photolysis.

While it is the case that arene exchange has only been shown to proceed for coordinated polyaromatics in  $[(\eta^6\text{-arene})\text{RuCp}]^+$  complexes, several alternative Ru complexes incorporating  $\eta^6$ -bound monoarenes have been shown to undergo arene exchange under photolytic conditions (Figure 13). Two examples are reported for complexes incorporating either phosphine (**59**)<sup>134</sup> or amidinate (**60**)<sup>135</sup> ligands. Iron dicarbollide complexes (**61**) have also been shown to undergo arene exchange under irradiation (100 W filament lamp) at a greater rate than  $[(\eta^6\text{-C}_6\text{H}_6)\text{FeCp}]\text{PF}_6$ .<sup>136</sup> Cobalt complexes with cyclobutadiene ligands can also undergo room temperature arene exchange. As with other examples, the rate of exchange depends upon the sterics of the outgoing arene and can be catalysed by coordinating solvents, such as acetone and MeCN. The complex  $[(\eta^6\text{-C}_6\text{H}_6)\text{CoCp}^*]^+$  (**62**) undergoes arene exchange with mesitylene two orders of magnitude slower than the analogous process with  $[(\eta^6\text{-C}_6\text{H}_6)\text{FeCp}]^+$ .<sup>137</sup>

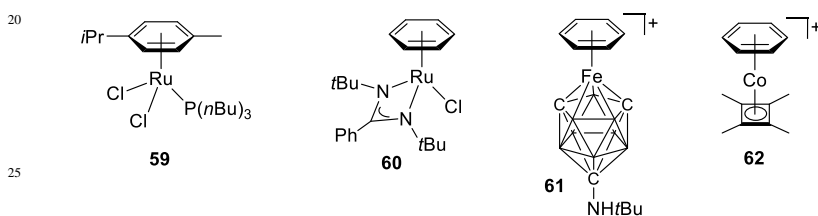


**Figure 13:** Selected metal-arene complexes that undergo photocatalytic arene exchange. In complex **61**, each unlabelled vertex in the cluster represents a BH unit.

The photochemical arene exchange in  $[(\eta^6\text{-arene})\text{Cr}(\text{CO})_3]$  complexes is feasible in some cases, but a competing process – loss of CO – hinders the use of this technique for arene exchange processes (Figure 14).<sup>138</sup> The nature of the coordinated arene has a large effect upon the two competing processes. When benzene is coordinated, only one excited state (a metal to CO charge transfer, MCCT, state) is reached upon photoexcitation at 400 nm, which leads to CO loss and no arene exchange (**63a**). When the coordinated arene is substituted (e.g., thioanisole),<sup>139</sup> the reduced symmetry allows for population of a second excited state (a metal to arene charge transfer, MACT, state) that promotes a ring slip process from  $\eta^6$  to  $\eta^4$  (**63b**), which subsequently leads to arene exchange. Arene exchange has a particularly high quantum yield when naphthalene is the coordinated arene, as was the case for  $[(\eta^6\text{-arene})\text{RuCp}]^+$  photocatalytic arene exchange.

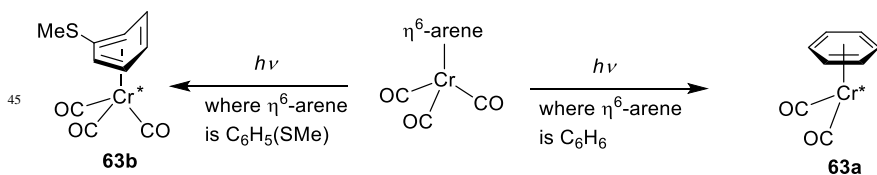


**Figure 14:** Photocatalytic reactions of  $[(\eta^6\text{-arene})\text{Cr}(\text{CO})_3]$  complexes.

A final point to consider is the source of light used to trigger arene exchange. In the majority of the examples discussed above, high-powered lamps are used to achieve arene exchange. We are yet to see an example of photocatalytic arene exchange using a simple LED set-up, as is commonly used in modern photocatalytic reactions. The practical utility of photolysis as a means to achieve catalytic reactions involving arene exchange will be greatly enhanced if such simple irradiation systems can be developed.

## 5 Catalytic Reactions via $\pi$ -arene Intermediates

As shown in previous sections,  $\pi$ -coordination of arenes to metals leads to enhanced reactivity. We have also seen that the ability of one aromatic group to exchange with a second is facilitated by solvent choice and UV irradiation. The key to achieving one-pot reactions that are catalytic in the activating metal fragment is to balance the reactivity of the metal-arene species with the ability to undergo arene exchange (Scheme 1). The challenge is that the properties that generally facilitate reactivity (strong metal-arene bonds with significant electron-withdrawing effects at the coordinated arene) tend to disfavour arene exchange. There are, however, several examples of successful reactions that are catalytic in the activating metal. In this section, we give a comprehensive review of these catalytic reactions. The reactions can be broken down into four classes:  $\pi$ -arene intermediates that subsequently undergo oxidative addition to the metal centre; reactions involving nucleophilic attack at the bound arene; reactions involving the benzylic or more distal positions of the coordinated arene; and photocatalytic reactions.

### 5.1 $\pi$ -Arene intermediates that subsequently undergo oxidative addition

The first class of catalytic reactions involves initial  $\eta^6$ -coordination of arenes to a metal centre, followed by an oxidative addition process. Although the mechanism was not determined until several years later, the first example of such a reaction came from Hartwig, who reported the nickel-catalysed hydrogenolysis of aryl ethers (Figure 15).<sup>140</sup> Hydrogenolysis typically involves high temperatures and pressure (e.g. 250 °C and 30 bar H<sub>2</sub>) or requires stoichiometric alkali metals. Inspired by previous reports of Ni(0)-catalysed C–O bond activation, Hartwig showed the successful hydrogenolysis of a variety of diaryl ethers and alkyl aryl ethers under 1 bar H<sub>2</sub>. The scope of the reaction was impressive, with both electron-rich and electron-poor arenes giving high yields, whilst showing no evidence for arene hydrogenation.

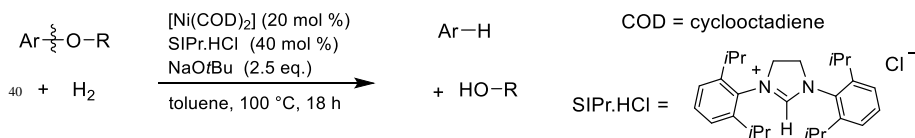


**Figure 15:** Catalytic hydrogenolysis of aryl ethers.

45



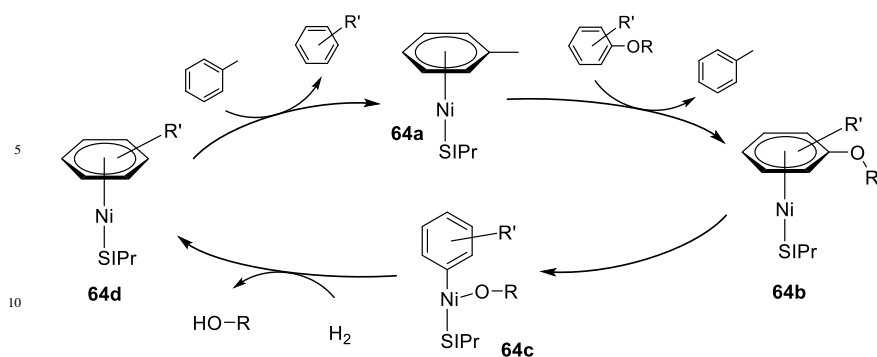


**Figure 16:** Mechanism for catalytic hydrogenolysis of aryl ethers.<sup>141</sup>

Several years later, a thorough investigation into the mechanism of hydrogenolysis was reported.<sup>141</sup> The proposed mechanism (Figure 16) goes via intermediate **64b**, which forms from arene exchange between  $[(\eta^6\text{-toluene})\text{Ni}(\text{SIPr})]$  (**64a**, SIPr is the *N*-heterocyclic carbene ligand produced from deprotonation of *N,N'*-(2,6-diisopropylphenyl)dihydroimidazolium), and Ar(R')OR. The η<sup>6</sup>-bound aryl ether then undergoes oxidative addition to give intermediate **64c**, followed by hydrogenolysis to give **64d**. Arene exchange between Ar(R') and toluene completes the catalytic cycle. Through detailed studies, it was shown that **64a** was the resting state for the catalysis and that arene exchange between this species and the aryl ether proceeds at room temperature within 30 minutes. A computational study on the step **64b**→**64c** suggested an η<sup>6</sup> to η<sup>2</sup> ring-slip prior to oxidative addition.<sup>142</sup> While no experimental evidence for such an intermediate has been presented, what is clear is that the η<sup>6</sup>-coordination of the arene to Ni is crucial for the subsequent bond cleavage. As further support for a mechanism involving the η<sup>6</sup>-arene intermediate, it was found that benzyl alkyl ethers, in which the ether functional group contains no directly-bound aromatic substituent, gave no reaction under the hydrogenolysis conditions. Such substrates could be activated by addition of AlMe<sub>3</sub>, but this process may well proceed via an alternative mechanism.

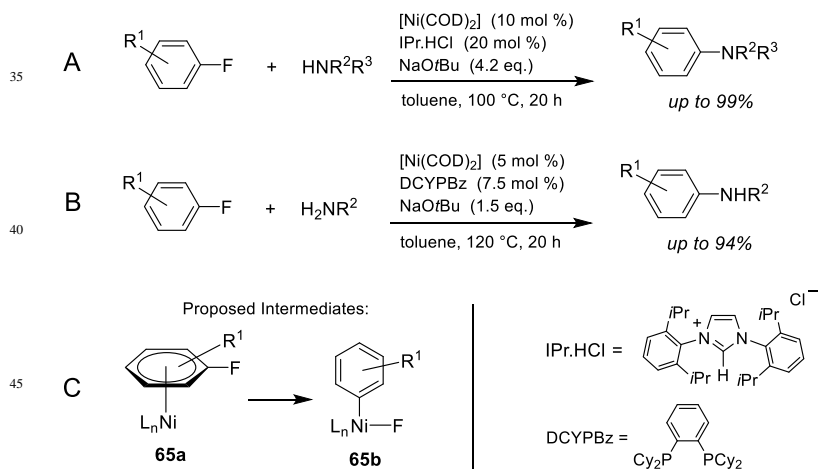


**Figure 17:** Catalytic reactions of arylfluorides via π-arene intermediates.

In the time between the initial report of Ni-catalysed hydrogenolysis and the subsequent mechanistic insight, Wang reported coupling of fluoroarenes with secondary amines, using closely-related catalytic conditions.<sup>143</sup> It was shown that coupling of a range of aromatic fluorides with various secondary amines proceeded with excellent yields, under the conditions shown in Figure 17A. While the mechanism of action was only briefly discussed, an oxidative addition of Ar–F to Ni(0) to give intermediate **65b** was proposed. With such similarity between the catalytic components of this reaction with Hartwig’s hydrogenolysis, it seems highly plausible that the Ar–F oxidative addition step is preceded by  $\eta^6$ -coordination of Ar–F to Ni(0) (**65a**, Figure 17C). Very recently, Iwai and Sawamura have extended this coupling reaction to include primary amines, by using alternative bulky bis-phosphine ligands in the place of NHC ligands (Figure 17B).<sup>144</sup>

While the previously discussed examples of aryl fluoride coupling reactions gave no direct evidence for  $\eta^6$ -arene intermediates, Bergman and Arnold have reported a catalytic hydrodefluorination of Ar–F compounds that is shown to proceed via an ( $\eta^6$ -arene)Nb<sup>III</sup> intermediate.<sup>145</sup> The overall reaction (Figure 18A) converts a small series of aryl fluorides to their hydrodefluorinated analogues with PhSiH<sub>3</sub> as the source of hydrogen, according to the mechanism shown in Figure 18B. It was found experimentally that reversible  $\eta^6$ -coordination of Ar–F precedes C–F bond activation. A detailed DFT study indicated that ( $\eta^6$ -ArF)Nb(III) intermediates (**66c**) undergo oxidative addition to intermediate **66a**, via a bimetallic arene-bridged inverted sandwich complex (**66d**), in accord with previous reports of such species.<sup>146</sup> Intermediate **66d** was calculated to have a lower energy reaction pathway than a mono-metallic complex undergoing oxidative addition.

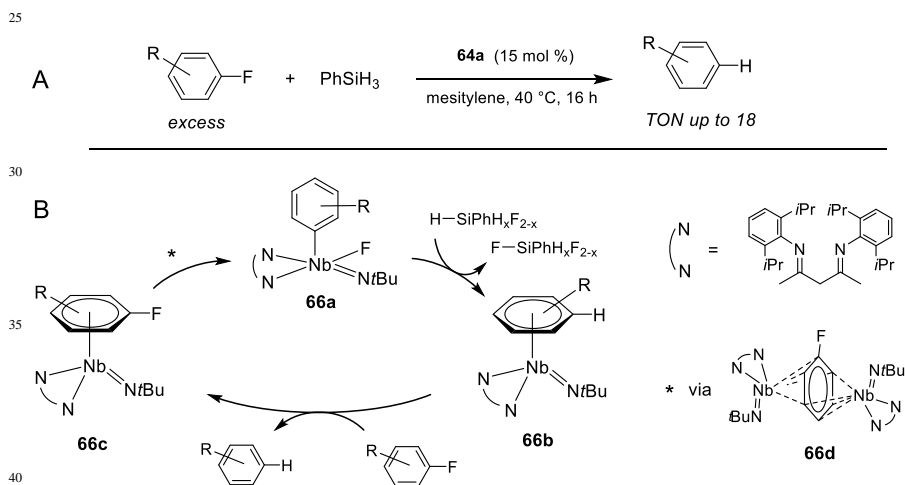
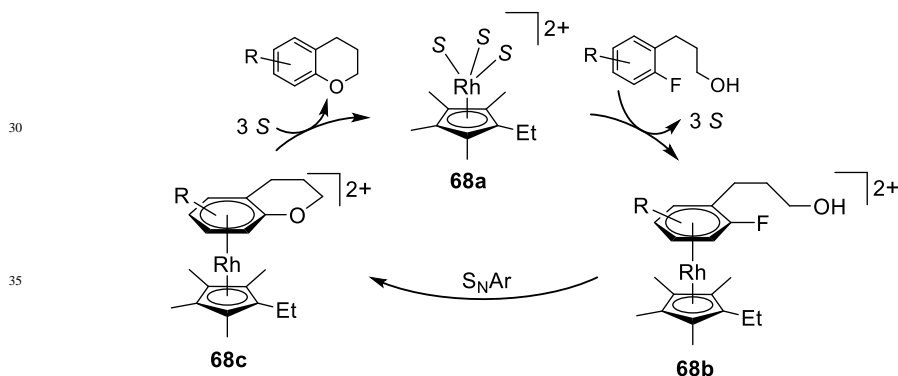
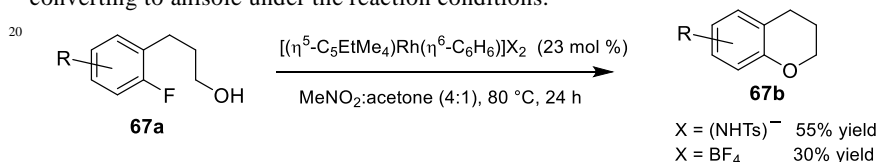


**Figure 18:** Nb-catalysed hydrodefluorination of arylfluorides.<sup>145</sup>

## 5.2 Catalytic reactions at $\pi$ -coordinated carbon centres

Several reactions have been reported in which catalytic quantities of metal complexes facilitate nucleophilic addition and substitution processes at aromatics via an  $\eta^6$ -arene intermediate. In 1980, Houghton reported the first example: an intramolecular cyclisation of 3-(2-fluorophenyl)-propanols (**67a**) to form chromans (**67b**) with catalytic  $[(\eta^6\text{-C}_6\text{H}_6)\text{Rh}(\eta^5\text{-C}_5\text{Me}_4\text{Et})]^{2+}$  (Scheme 18).<sup>147,148</sup> The reaction

proceeded with 23% catalyst loading in a mixed solvent system of MeNO<sub>2</sub>:acetone (4:1 v/v). On the basis of <sup>1</sup>H-NMR evidence, a catalytic mechanism was put forward (Figure 19) involving the formation of [S<sub>3</sub>Rh(η<sup>5</sup>-C<sub>5</sub>Me<sub>4</sub>Et)]<sup>2+</sup> (**68a**, where S = solvent), which subsequently formed the corresponding η<sup>6</sup>-fluoroarene complex **68b**, with loss of coordinating solvent. Intramolecular cyclisation is followed by displacement of η<sup>6</sup>-arene product for solvent to complete the catalytic cycle. Interestingly, the counter ion appeared to have a significant effect upon conversion with [PF<sub>6</sub>]<sup>-</sup> salts giving 55% conversion after 24 h and [BF<sub>4</sub>]<sup>-</sup> salts leading to only 30% reaction product. This effect was attributed to much faster arene dissociation for the [PF<sub>6</sub>]<sup>-</sup> salt, perhaps due to the formation of F<sup>-</sup> from anion decomposition under the reaction conditions, which can act as a catalyst for arene exchange. The reaction had a fairly limited substrate scope. While methoxy-substituted arenes proceeded to give product, nitro-substituted arenes gave no reaction product. Attempts to produce the 5-membered oxygen heterocycles from 2-(2-fluorophenyl)-ethanol were unsuccessful, as were the related amino or amido substrates. Despite this lack of generality, this reaction was the first example of catalysis via η<sup>6</sup>-arene intermediates. During this study, it was shown that intermolecular reactions were also feasible, with fluorobenzene and MeOH converting to anisole under the reaction conditions.



40

For more than 20 years this Rh-catalysed reaction remained the only example of its kind. However, in the past decade there has been a resurgence in the application of transient η<sup>6</sup>-arene intermediates in catalytic transformations. Shibata showed that nucleophilic aromatic substitution (S<sub>N</sub>Ar) of unactivated fluoroarenes (i.e. those without covalently-bound electron withdrawing groups) with secondary amine nucleophiles is facilitated by catalytic Ru species.<sup>149</sup> Initial reports employed a pre-catalyst system of [Ru(COD)(2-methylallyl)<sub>2</sub>], DPPent and TfOH (Figure 20). The reaction also included Et<sub>3</sub>SiH and Et<sub>3</sub>N to remove the HF by-product. The reaction required 5 equivalents of aryl fluoride relative to the amine nucleophile and

produced coupled products in up to 79% yield. Subsequent optimisation revealed a more bench-stable catalytic protocol with  $[\text{Ru}(\eta^6\text{-C}_6\text{H}_6)\text{Cl}_2]_2$ ,  $\text{AgOTf}$ ,  $\text{P}(p\text{-C}_6\text{H}_4\text{F})_3$  and molecular sieves, with yields above 80% for selected substrates.<sup>150</sup> Evidence for an  $\eta^6$ -arene catalytic mechanism was provided by *in situ*  $^1\text{H-NMR}$  and MS experiments, which revealed catalytic intermediate **69a** or **69b**, depending on the reaction conditions. Aryl chlorides and aryl bromides were not compatible with the catalytic reaction conditions, but were shown to successfully coordinative to Ru. This implies that in the general mechanism of catalytic nucleophilic substitution reactions (Figure 21)  $\text{S}_{\text{N}}\text{Ar}$  was rate limiting (**70a**  $\rightarrow$  **70b**) in the process rather than arene exchange. An increase in the rate of reaction for more electron withdrawing phosphine ligands,  $\text{P}(p\text{-C}_6\text{H}_4\text{F})_3 > \text{P}(p\text{-C}_6\text{H}_4\text{Me})_3 \sim \text{P}(p\text{-C}_6\text{H}_4\text{OMe})_3$ , is further evidence for rate limiting nucleophilic substitution.

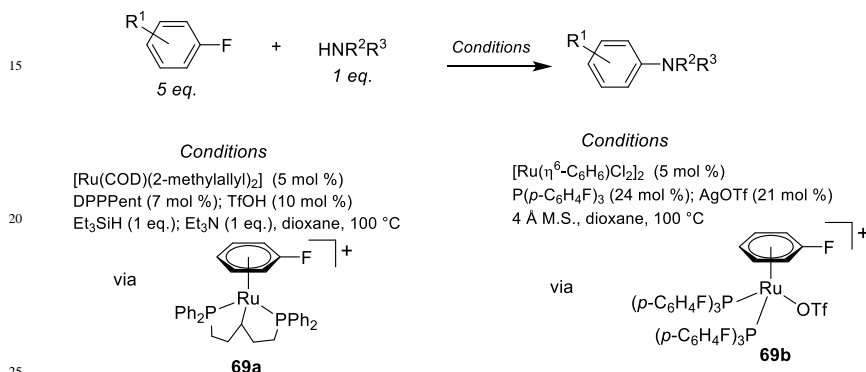


**Figure 20:** Ru-catalysed  $\text{S}_{\text{N}}\text{Ar}$  of aryl fluorides via  $\pi$ -arene intermediates.

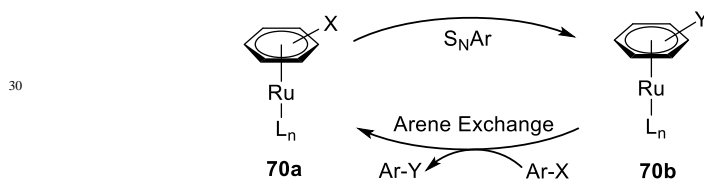


**Figure 21:** General mechanism for Ru-catalysed  $\text{S}_{\text{N}}\text{Ar}$  via  $\pi$ -arene intermediates.

Expanding the applicability of  $\eta^6$ -arene catalytic reactions, Walton reported the catalytic  $\text{S}_{\text{N}}\text{Ar}$  of aryl chlorides (Figure 22A), using an  $[(\eta^6\text{-}p\text{-cymene})\text{RuCp}]^+$  catalyst.<sup>32</sup> With 10 mol % catalyst, 4-chlorotoluene and morpholine were coupled in 90% yield in 1-octanol. The reaction showed a large dependence on solvent and temperature, with coordinating solvents and elevated temperature (up to 180 °C) giving higher conversions. These factors along with spectroscopic observation of  $\eta^6$ -coordinated reaction product revealed that arene exchange (**70b**  $\rightarrow$  **70a**, Figure 21) was rate limiting in the catalytic process. This is in contrast to the previous system in which the activation towards nucleophilic attack was rate limiting.

A related catalytic system was reported by Grushin for the fluorination of aryl chlorides with  $\text{CsF}$ , via  $[(\eta^6\text{-chloroarene})\text{RuCp}^*]^+$  intermediates (Figure 22B).<sup>151</sup> By employing the more electron rich  $\text{Cp}^*$  ligand, the fluorination of chlorobenzene was shown to proceed at 140 °C with catalytic turnover numbers of 4.2 in DMF, rising to 8.5 in neat chlorobenzene at 180 °C.

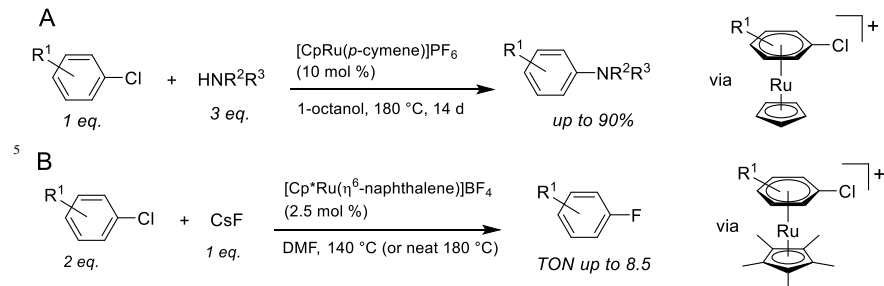


**Figure 22:** Ru-catalysed S<sub>N</sub>Ar of aryl chlorides via  $\pi$ -arene intermediates.

15
 A rare example of a main group metal-catalysis proceeding via a  $\pi$ -arene intermediate was reported by Tsuchimoto. The reaction shows S<sub>N</sub>Ar between a variety of indole nucleophiles and a methoxy thiophene, acting as the electrophile.<sup>152</sup> The reaction proceeds with catalytic [In(OTf)<sub>3</sub>] (2 – 10 mol %) to produce a wide range of bi-heterocyclic compounds (Figure 23A). The authors propose an  $\{(\eta^5\text{-thiophene})\text{In}\}$  intermediate (**71a**) in the catalytic cycle (Figure 23B), which activates the thiophene to nucleophilic attack by indole. Evidence for this

20
 mechanism comes from a deuterium labelling experiment in which deuterated indole reacts to give deuterium incorporation in the coupled thiophene ring. Such incorporation is only possible through the formation of In–C<sub>thiophene</sub> intermediate **71b**. Further evidence is proposed by the lack of reactivity of electron deficient thiophenes, which are less well-able to coordinate to the In(III) activating metal. In a

25
 more recent study, the authors have also shown that methoxy thiophenes can react with a wide range of amine, alcohol and sulfur-derived nucleophiles, under similar indium-catalysed conditions.<sup>153</sup> Similar indium  $\pi$ -arene intermediates have been implicated in the catalysed formation of heteroarylquinolines.<sup>154</sup>

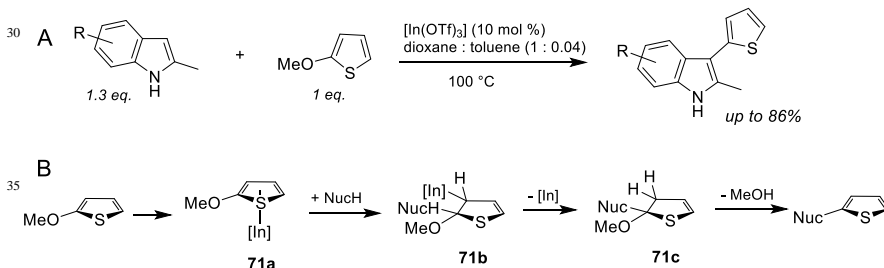


**Figure 23:** In-catalysed S<sub>N</sub>Ar of methoxythiophenes via a  $\pi$ -arene intermediate.<sup>152</sup>

40

### 5.3 Reactions at the benzylic or more distal positions

45
 While the previous catalytic reactions involved changes to substrates at the carbon atoms bound to the metal centre, transformations at more distal centres can also be facilitated by the  $\eta^6$ -coordination of arenes to a metal centre. It has been long-established that benzylic protons become more acidic upon arene coordination to selected metal complexes.<sup>155</sup> Matsuzaka and Takemoto recently showed condensation of toluene and aromatic aldehydes to form stilbene derivatives in high yields with catalytic  $[(\eta^6\text{-toluene})\text{RuCp}^*]^+$  (Figure 24A).<sup>156</sup> The reaction involves

initial deprotonation at the benzylic position of  $\eta^6$ -bound toluene to give intermediate **72b** (Figure 24B).  $\pi$ -Coordination stabilises the deprotonated intermediate, which subsequently reacts with the electrophilic aldehyde, which itself is pre-activated by imine formation (**72c**) with the [NHTs]<sup>-</sup> counterion. Elimination of the [NHTs]<sup>-</sup> counterion from **72d** yields the  $\eta^6$ -coordinated stilbene product (**72e**), which undergoes arene exchange with toluene to complete the catalytic cycle. The important role of the counter ion in imine formation from the starting aldehyde was confirmed by the absence of reactivity with Cl<sup>-</sup> or [TfO]<sup>-</sup> salts. Further evidence comes from the successful reaction of pre-formed imine starting material. While details of the rate limiting step in this process were not provided, it is plausible that the final arene exchange step is rate limiting, in accordance with previous catalytic reactions. Indirect evidence comes from the lower reactivity when the less electron rich [ $\eta^6$ -toluene]RuCp<sup>+</sup> catalyst is employed, which would be expected to show slower arene exchange. The significant increase in yield at higher temperature and longer reaction times (130 °C, 4 h: 50% yield versus 150 °C, 24 h: 98% yield) may also imply rate limiting arene exchange. The reaction was extended to xylene condensation with aryl aldehydes, which led to distyrylbenzene derivatives in good to excellent yields.

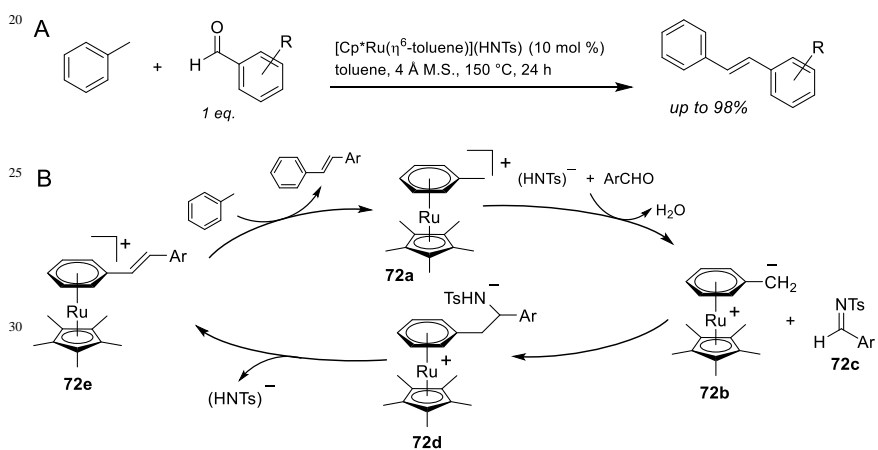


**Figure 24:** Ru-catalysed benzylic functionalisation of  $\pi$ -coordinated toluene.<sup>156</sup>

A final example of catalytic reactions involving transient  $\pi$ -arene species is the anti-Markovnikov addition of nucleophiles to styrene derivatives. Hartwig was the first to report the reaction between a range of styrene derivatives with secondary amines (Figure 25A).<sup>157</sup> By tuning the phosphine ligand used, regioselective addition to the beta position of styrene was achieved in overall 96% yield, owing to the stabilisation of negative charge in the alpha position when styrene is  $\pi$ -coordinated. A range of styrene and secondary amines were reacted in high yields. The mechanism of this reaction was deduced to proceed via intermediate **73a** (Figure 25C),<sup>158</sup> which was isolated from reaction between [Ru(COD)(2-methylallyl)<sub>2</sub>], DPPPEnt and styrene. Intermediate **73a** was shown to be competent in the catalytic cycle. This species was also shown undergo stoichiometric reaction with morpholine to generate the  $\eta^6$ -bound product **73b** with a rate constant of  $k_{\text{obs}} = 5.6 \times 10^{-3} \text{ s}^{-1}$ . Furthermore, the arene exchange between the

bound product and styrene was shown to proceed with a rate constant of  $k_{\text{obs}} = 5.6 \times 10^{-3} \text{ s}^{-1}$ . The similarity in rate constants illustrates the importance of the balance between the rate of reaction and rate of arene exchange. For successful catalytic procedures each process must take place under the reaction conditions and an important challenge for future reactions is to balance these two parameters. As a further development to this reaction, Shibata explored the use of chiral bis-phosphine ligands to impart enantioselectivity on the reaction products of  $\alpha$ -methyl styrene addition.<sup>159</sup> With the ligand (*S*)-xylylBINAP, 76% ee was achieved, albeit with overall lower reaction yield (Figure 25B).

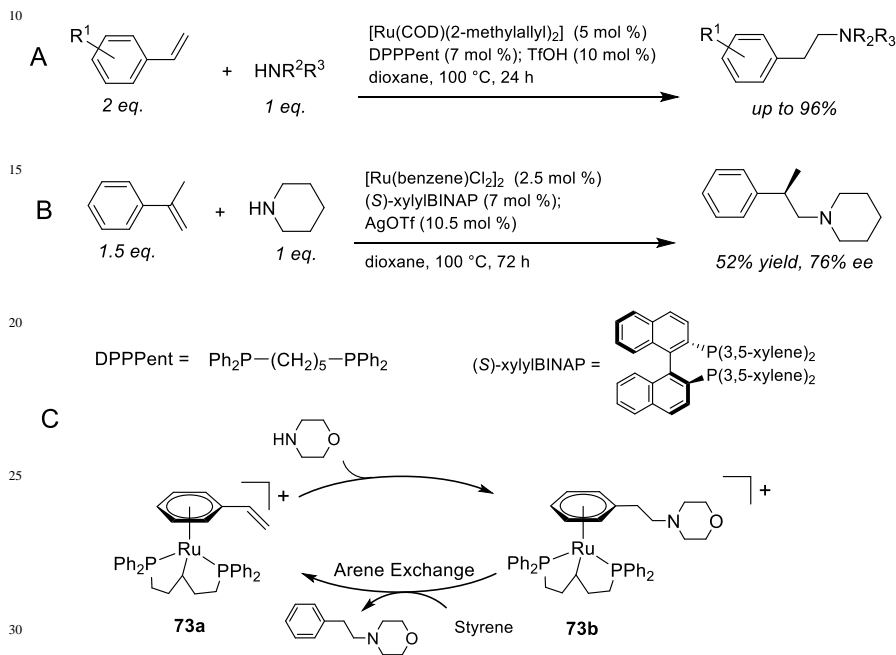


**Figure 25:** Ru-catalysed anti-Markovnikov addition of nucleophiles to  $\pi$ -coordinated styrene.

#### 5.4 Photocatalytic Reactions

As discussed in the previous section, photo-irradiation can be used to trigger arene exchange reactions. A single example of a photocatalytic reaction that proceeds via an  $\eta^6$ -arene intermediate has been reported.<sup>160</sup> The reaction is an enediyne cycloaromatisation. Initially it was found that **74** undergoes a Bergman cycloaromatisation<sup>161</sup> with stoichiometric  $[(\text{MeCN})_3\text{MCp}^*]^+$  ( $\text{M} = \text{Fe}$  or  $\text{Ru}$ ) and  $\gamma$ -terpene as the H-atom source to give  $[(\eta^6\text{-C}_6\text{H}_4(i\text{Pr})_2)\text{MCp}^*]^+$ . Liberation of the  $\eta^6$ -bound arene was carried out under photolytic conditions (medium pressure 500 W Hanovia lamp) in MeCN. It was shown that the reaction could also be carried out using catalytic metal under constant irradiation (Figure 26A). The mechanism is believed to proceed via in situ liberation of the  $\eta^6$ -bound product to give intermediate **75a**, which can go on to produce further equivalents of the cycloaromatisation product (Figure 26B). When  $[(\eta^6\text{-C}_6\text{H}_4(i\text{Pr})_2)\text{FeCp}^*]^+$  is used as the catalytic species, the reaction proceeded to 91% yield with a turnover number of 3.3. The Ru analogues gave slightly lower yields. Despite the low turnover number

in this reaction, it is a landmark study that shows the potential for combining activating  $\pi$ -arene metal complexes and photocatalytic arene exchange to achieve catalytic reactions.

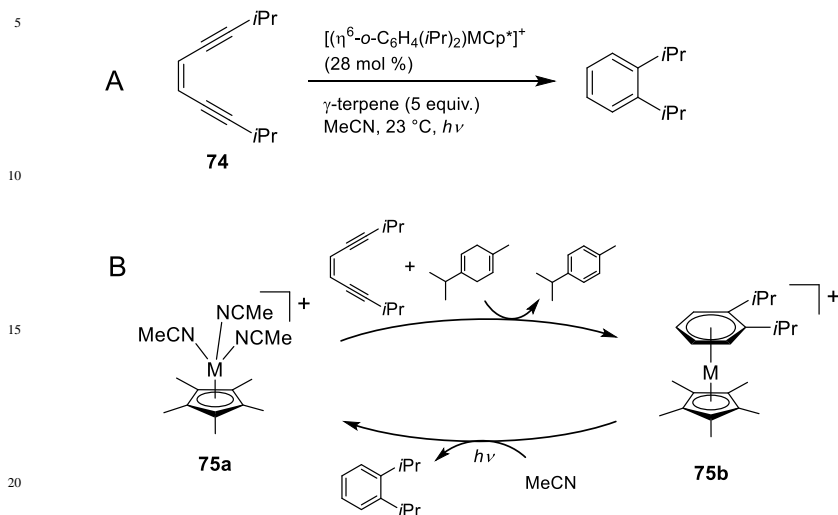


**Figure 26:** Photocatalytic cycloaromatisation via  $\pi$ -arene metal intermediates (M = Ru(II) or Fe(II)).<sup>160</sup>

## 6 Conclusions and Outlook

25 The purpose of this review has been to highlight the great potential for catalytic reactions involving  $\pi$ -arene intermediates. While fundamental knowledge of the behaviour of  $\pi$ -arene complexes has been described for more than 50 years, there has been a recent resurgence in the development of these systems, with an emphasis on catalytic reactions. The advantages of employing  $\pi$ -arene intermediates in catalytic

30 reactions are the increase in arene electrophilicity and C-H bond acidity upon coordination. The metal itself also provides a steric shield, leading to potential stereoselective reactions. Modulation of arene reactivity extends beyond the coordinated atoms to the benzylic positions and even more distal sites. Taking advantages of these features, there have been a host of contemporary reactions

35 reported recently of stoichiometric and catalytic  $\pi$ -arene metal complexes, as summarised in this review.

For such reactions to be truly transformative, the next step needs to be the focus on the development of catalytic reactions with greatly enhanced turnover numbers. To compete with the most efficient catalytic reaction, TON need to move to the 100s

40 and 1000s. The synthesis of new classes of metal-arene complexes may lead to the desired increase in reaction efficiency. The key to maximising TON is to balance reactivity of the bound arene with the rate of arene exchange. As Hartwig showed in the development of catalytic addition to styrenes, matching the rates of these two processes is crucial to achieving catalysis. In future studies, more emphasis should

45 be placed on the kinetic analysis of these two factors.

A major challenge to catalytic reactions is that the factors causing reactivity of coordinated arenes (namely, strong metal-arene bonds with significant  $\pi$ -bonding)



tend to disfavour the arene exchange process. A second issue is that in certain cases (e.g. catalytic nucleophilic substitution of aryl halides) the  $\pi$ -bound product is more thermodynamically stable than the  $\pi$ -bound starting material, making the arene exchange process particularly challenging. Judicious choice of reagents can circumvent such problems, but in order to produce general reactions, a step-change in the catalytic method is needed. This may well arise from the use of photocatalysis, which has become widespread in the modern era of catalysis. The use of light to facilitate arene exchange in catalytic  $\pi$ -arene reactions could lead to a paradigm shift in this reaction class. While a single example of such systems has been published, we feel that development in this area could transform the field. Whether the next generation of  $\pi$ -arene catalytic reaction is photocatalysed or not, there is clearly huge potential for catalytic reactions proceeding via  $\pi$ -arene intermediates and with the recent flurry of catalytic examples being published, we envisage great progress in this field in the coming years.

## 7 References

- 1 P. E. Kündig, Ed., *Transition Metal Arene Pi-Complexes in Organic Synthesis and Catalysis*, Springer, 1st edn., 2004.
- 2 J. T. Lyon and L. Andrews, *J. Phys. Chem. A*, 2006, **110**, 7806–7815.
- 3 F. A. Cotton, P. A. Kibala and W. A. Wojtczak, *J. Am. Chem. Soc.*, 1991, **113**, 1462–1463.
- 4 Y. Nakanishi, Y. Ishida and H. Kawaguchi, *Dalton Trans.*, 2016, **45**, 15879–15885.
- 5 A. F. R. Kilpatrick, J. C. Green, Z. R. Turner, J.-C. Buffet and D. O'Hare, *Chem. Commun.*, 2017, **53**, 12048–12051.
- 6 H. Braunschweig, C. Brückner, M. A. Celik, K. Dück, F. Hupp, T. Kramer, J. Krebs and I. Krummenacher, *Chem. Eur. J.*, 2015, **21**, 11056–11064.
- 7 L. Calucci, U. Englert, G. Pampaloni, C. Pinzino and M. Volpe, *J. Organomet. Chem.*, 2005, **690**, 4844–4855.
- 8 F. Marchetti, G. Pampaloni and C. Pinzino, *J. Organomet. Chem.*, 2006, **691**, 3458–3463.
- 9 R. Choukroun, C. Lorber and L. Vendier, *Organometallics*, 2007, **26**, 3604–3606.
- 10 N. Parvin, S. Pal, J. Echeverria, S. Alvarez and S. Khan, *Chem. Sci.*, 2017, **8**, 3249–3253.
- 11 M. Tamm, T. Bannenberg, R. Frohlich, S. Grimme and M. Gerenkamp, *Dalton Trans.*, 2004, 482–491.
- 12 E. P. Kündig, C. H. Fabritius, G. Grossheimann, P. Romanens, H. Butenschön and H. G. Wey, *Organometallics*, 2004, **23**, 3741–3744.
- 13 C. (Xiang) Lee, E. A. Pedrick and N. E. Leadbeater, *J. Flow Chem.*, 2012, **2**, 115–117.
- 14 C. Bolm and K. Muñiz, *Chem. Soc. Rev.*, 1999, **28**, 51–59.
- 15 C. Wilson-Konderka, K. Doxtator and C. Metallinos, *Adv. Synth. Cat.*, 2016, **358**, 2599–2603.
- 16 T. Ziegler and U. Heber, *Beilstein J. Org. Chem.*, 2012, **8**, 1059–1070.
- 17 S. Antonini, F. Calderazzo, U. Englert, E. Grigiotti, G. Pampaloni and P. Zanello, *J. Organomet. Chem.*, 2004, **689**, 2158–2168.
- 18 M. Tamm, T. Bannenberg, B. Dressel, R. Fröhlich and D. Kunz, *Organometallics*, 2001, **20**, 900–904.
- 19 Y. Ning, A. A. Sarjeant, C. L. Stern, T. H. Peterson and S. T. Nguyen, *Inorg. Chem.*, 2012, **51**, 3051–3058.
- 20 J. D. Jackson, S. J. Villa, D. S. Bacon, R. D. Pike and G. B. Carpenter, *Organometallics*,

- 1994, **13**, 3972–3980.
- 21 W. Dai, S. B. Kim, R. D. Pike, C. L. Cahill and D. A. Sweigart, *Organometallics*, 2010, **29**, 5173–5178.
- 22 G. Pampaloni, *Coord. Chem. Rev.*, 2010, **254**, 402–419.
- 5 23 E. A. Trifonova, D. S. Perekalin, K. A. Lyssenko and A. R. Kudinov, *J. Organomet. Chem.*, 2013, **727**, 60–63.
- 24 G. Meola, H. Braband, D. Hernández-Valdés, C. Gotzmann, T. Fox, B. Spingler and R. Alberto, *Inorg. Chem.*, 2017, **56**, 6297–6301.
- 25 G. Meola, H. Braband, S. Jordi, T. Fox, O. Blacque, B. Spingler and R. Alberto, *Dalton Trans.*, 2017, **46**, 14631–14637.
- 10 26 M. Benz, H. Braband, P. Schmutz, J. Halter and R. Alberto, *Chem. Sci.*, 2015, **6**, 165–169.
- 27 E. P. Kündig, P. Jeger and G. Bernardinelli, *Inorg. Chim. Acta*, 2004, **357**, 1909–1919.
- 28 M. Driess, M. P. Luecke, D. Porwal, A. Kostenko, Y. Zhou, S. Yao, M. Keck, C. Limberg and M. Oestreich, *Dalton Trans.*, 2017, **46**, 16412–16418.
- 15 29 P. Kumar, R. K. Gupta and D. S. Pandey, *Chem. Soc. Rev.*, 2014, **43**, 707–733.
- 30 J. M. Cross, T. R. Blower, N. Gallagher, J. H. Gill, K. L. Rockley and J. W. Walton, *ChemPlusChem*, 2016, **81**, 1276–1280.
- 31 B. M. Trost and C. M. Older, *Organometallics*, 2002, **21**, 2544–2546.
- 32 J. W. Walton and J. M. J. Williams, *Chem. Commun.*, 2015, **51**, 2786–2789.
- 20 33 E. Kayahara, V. K. Patel, A. Mercier, E. P. Kündig and S. Yamago, *Angew. Chem. Int. Ed.*, 2016, **55**, 302–306.
- 34 T. Shibusaki, N. Komine, M. Hirano and S. Komiya, *Organometallics*, 2006, **25**, 523–527.
- 35 E. E. Karslyan, A. O. Borissova and D. S. Perekalin, *Angew. Chem. Int. Ed.*, 2017, **56**, 5584–5587.
- 25 36 E. E. Karslyan, D. S. Perekalin, P. V. Petrovskii, A. O. Borisova and A. R. Kudinov, *Russ. Chem. Bull.*, 2009, **58**, 585–588.
- 37 R. Soni, K. E. Jolley, G. J. Clarkson and M. Wills, *Org. Lett.*, 2013, **15**, 5110–5113.
- 38 H. Boennemann, R. Goddard, J. Grub, R. Mynott, E. Raabe and S. Wendel, *Organometallics*, 1989, **8**, 1941–1958.
- 30 39 G. Großheimann, S. Holle and P. W. Jolly, *J. Organomet. Chem.*, 1998, **568**, 205–211.
- 40 A. R. Kudinov, E. V. Mutseneck and D. A. Loginov, *Coord. Chem. Rev.*, 2004, **248**, 571–585.
- 41 D. A. Loginov, A. A. Pronin, Z. A. Starikova, A. V. Vologzhanina, P. V. Petrovskii and A. R. Kudinov, *Eur. J. Inorg. Chem.*, 2011, 5422–5429.
- 35 42 D. V. Muratov, A. S. Romanov, D. A. Loginov, M. Corsini, F. Fabrizi De Biani and A. R. Kudinov, *Eur. J. Inorg. Chem.*, 2015, 804–816.
- 43 S. D. Pike, A. L. Thompson, A. G. Algara, D. C. Apperley, S. A. Macgregor and A. S. Weller, *Science*, 2012, **337**, 1648–1652.
- 44 S. D. Pike, M. R. Crimmin and A. B. Chaplin, *Chem. Commun.*, 2017, **53**, 3615–3633.
- 40 45 N. V. Shvydkiy, E. A. Trifonova, A. M. Shved, Y. V. Nelyubina, D. Chusov, D. S. Perekalin and A. R. Kudinov, *Organometallics*, 2016, **35**, 3025–3031.
- 46 A. Meltzer, C. Präsang, C. Milsmann and M. Driess, *Angew. Chem. Int. Ed.*, 2009, **48**, 3170–3173.
- 47 C. Watanabe, Y. Inagawa, T. Iwamoto and M. Kira, *Dalton Trans.*, 2010, **39**, 9414–9420.
- 45 48 Y. Hoshimoto, Y. Hayashi, H. Suzuki, M. Ohashi and S. Ogoshi, *Organometallics*, 2014, **33**, 1276–1282.
- 49 T. Nickel, R. Goddard and C. Kruger, *Angew. Chem. Int. Ed.*, 1994, **33**, 879–882.

- 50 C. A. Laskowski, A. J. M. Miller, G. L. Hillhouse and T. R. Cundari, *J. Am. Chem. Soc.*, 2011, **133**, 771–773.
- 51 H. L. Chang, D. S. Laitar, P. Mueller and J. P. Sadighi, *J. Am. Chem. Soc.*, 2007, **129**, 13802–13803.
- 52 A. M. Wright, G. Wu and T. W. Hayton, *Inorg. Chem.*, 2011, **50**, 11746–11753.
- 53 S. Zhu, M. M. Shoshani and S. A. Johnson, *Chem. Commun.*, 2017, **53**, 13176–13179.
- 54 R. G. Gastinger and K. J. Klabunde, *Transit. Met. Chem.*, 1979, **4**, 1–13.
- 55 R. G. Gastinger, B. B. Anderson and K. J. Klabunde, *J. Am. Chem. Soc.*, 1980, **102**, 4959–4966.
- 56 T. J. Groshens and K. J. Klabunde, *Organometallics*, 1982, **1**, 564–565.
- 57 C. Juan, M. L. Reyes, E. Passaglia and C. S. Pisa, *Chem. Commun.*, 2003, 78–79.
- 58 A. R. O'Connor, P. S. White and M. Brookhart, *Organometallics*, 2010, **29**, 5382–5389.
- 59 A. R. O. Connor, S. A. Urbin, R. A. Moorhouse, P. S. White and M. Brookhart, *Organometallics*, 2009, **28**, 2372–2384.
- 60 G. E. Herberich, U. Englert and F. Marken, *J. Chem. Soc., Dalt. Trans.*, 1993, **8**, 4–7.
- 61 B. Thapaliya, S. Debnath, N. Arulsamy and D. M. Roddick, *Organometallics*, 2015, **34**, 4018–4022.
- 62 M. Rosillo, G. Domínguez and J. Pérez-Castells, *Chem. Soc. Rev.*, 2007, **36**, 1589–1604.
- 63 M. Lafrance, C. N. Rowley, T. K. Woo and K. Fagnou, *J. Am. Chem. Soc.*, 2006, **128**, 8754–8756.
- 64 P. Ricci, K. Krämer, X. C. Cambeiro and I. Larrosa, *J. Am. Chem. Soc.*, 2013, **135**, 13258–13261.
- 65 D. Whitaker, J. Burés and I. Larrosa, *J. Am. Chem. Soc.*, 2016, **138**, 8384–8387.
- 66 P. Ricci, K. Krämer and I. Larrosa, *J. Am. Chem. Soc.*, 2014, **136**, 18082–18086.
- 67 L. A. Wilkinson, J. A. Pike and J. W. Walton, *Organometallics*, 2017, **36**, 4376–4381.
- 68 E. M. D'Amato, C. N. Neumann and T. Ritter, *Organometallics*, 2015, **34**, 4626–4631.
- 69 K. Kamikawa, S. Kinoshita, M. Furusyo, S. Takemoto, H. Matsuzaka and M. Uemura, *J. Org. Chem.*, 2006, **72**, 2001–2004.
- 70 A. J. Pearson and H. Shin, *J. Org. Chem.*, 1994, **59**, 2314–2323.
- 71 A. J. Pearson, J. G. Park and P. Y. Zhu, *J. Org. Chem.*, 1992, **57**, 3583–3589.
- 72 A. J. Pearson, J. G. Park, S. H. Yang and Y. Chuang, *J. Chem. Soc. Chem. Commun.*, 1989, 1363–1364.
- 73 R. C. Cambie, S. J. Janssen, P. S. Rutledge and P. D. Woodgate, *J. Organomet. Chem.*, 1991, **420**, 387–418.
- 74 R. C. Cambie, G. R. Clark, S. L. Coombe, S. A. Coulson, P. S. Rutledge and P. D. Woodgate, *J. Organomet. Chem.*, 1996, **507**, 1–21.
- 75 M. H. Beyzavi, D. Mandal, M. G. Strebl, C. N. Neumann, E. M. D'Amato, J. Chen, J. M. Hooker and T. Ritter, *ACS Cent. Sci.*, 2017, **3**, 944–948.
- 76 C. N. Neumann, J. M. Hooker and T. Ritter, *Nature*, 2016, **538**, 274–274.
- 77 T. Furuya, A. S. Kamlet and T. Ritter, *Nature*, 2011, **473**, 470–477.
- 78 J. A. Pike and J. W. Walton, *Chem. Commun.*, 2017, **53**, 9858–9861.
- 79 M. Makosza and K. Wojciechowski, *Top. Heterocycl. Chem.*, 2014, **37**, 51–106.
- 80 F. Rose-Munch, A. Marti, D. Cetiner, J.-P. Tranchier and E. Rose, *Dalton Trans.*, 2011, **40**, 1567–1575.
- 81 W. H. Miles, C. M. Madison, C. Y. Kim, D. J. Sweitzer, S. D. Valent and D. M. Thamattoor, *J. Organomet. Chem.*, 2017, **851**, 218–224.
- 82 P. E. Kündig, C. H. Fabritius, G. Grossheimann, F. Robvieux, P. Romanens and G.

- Bernardinelli, *Angew. Chem. Int. Ed.*, 2002, **41**, 4577–4579.
- 83 S. Shirakawa, K. Yamamoto and K. Maruoka, *Angew. Chem. Int. Ed.*, 2015, **54**, 838–840.
- 84 D. Whitaker, M. Batuecas, P. Ricci and I. Larrosa, *Chem. Eur. J.*, 2017, **23**, 12763–12766.
- 85 J. A. Heppert, M. A. Morgenstern, D. M. Scherubel, F. Takusagawa and M. R. Shaker,
- 5 *Organometallics*, 1988, **7**, 1715–1723.
- 86 J. A. Heppert, M. E. Thomas-Miller, P. N. Swepston and M. W. Extine, *J. Chem. Soc., Chem. Commun.*, 1988, 280–282.
- 87 P. K. Sazonov, V. A. Ivushkin, V. N. Khrustalev, N. G. Kolotyrykina and I. P. Beletskaya, *Dalton Trans.*, 2014, **43**, 13392–13398.
- 10 88 J. A. Heppert, M. E. Thomas-Miller, D. M. Scherubel, F. Takusagawa, M. A. Morgenstern and M. R. Shaker, *Organometallics*, 1989, **8**, 1199–1206.
- 89 S. Chen, V. Carperos, B. Noll, R. J. Swope and M. R. DuBois, *Organometallics*, 1995, **14**, 1221–1231.
- 90 A. Schlüter, K. Bieber and W. S. Sheldrick, *Inorg. Chim. Acta*, 2002, **340**, 35–43.
- 15 91 D. Astruc, Y. Wang, A. Rapakousiou, A. Diallo, R. Djeda, J. Ruiz and C. Ornelas, *Polyhedron*, 2015, **86**, 24–30.
- 92 F. Moulines, L. Djakovitch, R. Boese, B. Gloaguen, W. Thiel, J.-L. Fillaut, M.-H. Deville and D. Astruc, *Angew. Chem. Int. Ed.*, 1993, **32**, 1075–1077.
- 93 D. Morvan, T. B. Rauchfuss and S. R. Wilson, *Organometallics*, 2009, **28**, 3161–3166.
- 20 94 B. T. Loughrey, M. L. Williams, P. G. Parsons and P. C. Healy, *J. Organomet. Chem.*, 2016, **819**, 1–10.
- 95 W. Strohmeier and H. Mittnacht, *Z. Phys. Chem.*, 1963, **38**, 315–325.
- 96 E. L. Muetterties, J. R. Bleeke and A. C. Sievert, *J. Organomet. Chem.*, 1979, **178**, 197–216.
- 25 97 T. G. Traylor, K. J. Stewart and M. J. Goldberg, *J. Am. Chem. Soc.*, 1984, **106**, 4445–4454.
- 98 C. A. L. Mahaffy and P. L. Pauson, *J. Chem. Res. Synop.*, 1979, **126**, 1752–1775.
- 99 C. L. Zimmerman, S. L. Shaner, S. A. Roth and B. R. Willeford, *J. Chem. Res. Synop.*, 1980, **108**, 1289–1297.
- 30 100 W. Strohmeier and H. Mittnacht, *Z. Phys. Chem.*, 1961, **29**, 339–346.
- 101 B. R. Jagirdar and K. J. Klabunde, *J. Coord. Chem.*, 1995, **34**, 31–43.
- 102 D. S. Perekalin and A. R. Kudinov, *Coord. Chem. Rev.*, 2014, **276**, 153–173.
- 103 A. I. Konovalov, E. E. Karslyan, D. S. Perekalin, Y. V. Nelyubina, P. V. Petrovskii and A. R. Kudinov, *Mendeleev Commun.*, 2011, **21**, 163–164.
- 35 104 T. Shibusaki, N. Komine, M. Hirano and S. Komiya, *J. Organomet. Chem.*, 2007, **692**, 2385–2394.
- 105 D. S. Perekalin, E. E. Karslyan, P. V. Petrovskii, A. O. Borissova, K. A. Lyssenko and A. R. Kudinov, *Eur. J. Inorg. Chem.*, 2012, 1485–1492.
- 106 M. Rioja, P. Hamon, T. Roisnel, S. Sinbandhit, M. Fuentealba, K. Letelier, J.-Y. Saillard,
- 40 A. Vega and J.-R. Hamon, *Dalton Trans.*, 2015, **44**, 316–329.
- 107 J. M. Lynam, L. M. Milner, N. S. Mistry, J. M. Slattery, S. R. Warrington and A. C. Whitwood, *Dalton Trans.*, 2014, **43**, 4565–4572.
- 108 R. Makhoul, J. A. Shaw-Taberlet, H. Sahnoune, V. Dorcet, S. Kahlal, J. F. Halet, J. R. Hamon and C. Lapinte, *Organometallics*, 2014, **33**, 6023–6032.
- 45 109 A. Decken, J. F. Britten and M. J. McGlinchey, *J. Am. Chem. Soc.*, 1993, **115**, 7275–7284.
- 110 E. T. Singewald, X. Shi, C. A. Mirkin, S. J. Schofer and C. L. Stern, *Organometallics*, 1996, **15**, 3062–3069.

- 111 H. Tobita, K. Hasegawa, J. J. G. Minglana, L. S. Luh, M. Okazaki and H. Ogino, *Organometallics*, 1999, **18**, 2058–2060.
- 112 M.-P. Luecke, D. Porwal, A. Kostenko, Y.-P. Zhou, S. Yao, M. Keck, C. Limberg, M. Oestreich and M. Driess, *Dalton Trans.*, 2017, **46**, 16412–16418.
- 5 113 A. Meltzer, C. Präsang, C. Milsmann and M. Driess, *Angew. Chem. Int. Ed.*, 2009, **48**, 3170–3173.
- 114 R. G. Gastinger, B. B. Anderson and K. J. Klabunde, *J. Am. Chem. Soc.*, 1980, **102**, 4959–4966.
- 115 S. L. Mukerjee, R. F. Lang, T. Ju, G. Kiss and C. D. Hoff, *Inorg. Chem.*, 1992, **31**, 4885–  
10 4889.
- 116 M. Al-Afyouni, A. Kayser, F. Hung-Low, J. W. Tye and C. A. Bradley, *Polyhedron*, 2016, **114**, 385–392.
- 117 B. Thapaliya, S. Debnath, N. Arulsamy and D. M. Roddick, *Organometallics*, 2015, **34**, 4018–4022.
- 15 118 A. R. O'Connor, S. A. Urbin, R. A. Moorhouse, P. S. White and M. Brookhart, *Organometallics*, 2009, **28**, 2372–2384.
- 119 P. G. Hayes, W. E. Piers and M. Parvez, *Chem. Eur. J.*, 2007, **13**, 2632–2640.
- 120 E. P. Kündig, M. Kondratenko and P. Romanens, *Angew. Chem. Int. Ed.*, 1998, **37**, 3146–3148.
- 20 121 M. F. Semmelhack, A. Chlenov, L. Wu and D. Ho, *J. Am. Chem. Soc.*, 2001, **123**, 8438–8439.
- 122 R. Soni, K. E. Jolley, G. J. Clarkson and M. Wills, *Org. Lett.*, 2013, **15**, 5110–5113.
- 123 A. J. Pearson, J. G. Park, S. H. Yang and Y. Chuang, *J. Chem. Soc. Chem. Commun.*, 1989, 10–11.
- 25 124 R. J. Lavallee and C. Kutal, *J. Organomet. Chem.*, 1998, **562**, 97–104.
- 125 R. C. Cambie, G. R. Clark, S. L. Coombe, S. A. Coulson, P. S. Rutledge and P. D. Woodgate, *J. Organomet. Chem.*, 2006, **55**, 2247–2255.
- 126 A. M. McNair, J. L. Schrenk and K. R. Mann, *Inorg. Chem.*, 1984, **23**, 2633–2640.
- 127 T. P. Gill and K. R. Mann, *Inorg. Chem.*, 1983, **22**, 1986–1991.
- 30 128 T. P. Gill and K. R. Mann, *Inorg. Chem.*, 1980, **19**, 3007–3010.
- 129 M. G. Choi, T. C. Ho and R. J. Angelici, *Organometallics*, 2008, **27**, 1098–1105.
- 130 E. E. Karslyan, D. S. Perekalin, P. V Petrovskii, A. O. Borisova and A. R. Kudinov, *Russ. Chem. Bull. Int. Ed.*, 2009, **58**, 585–588.
- 131 K. R. Mann, A. M. Blough, J. L. Schrenk, R. S. Koefod, D. A. Freedman and J. R. Matachek, *Pure Appl. Chem.*, 1995, **67**, 95–101.
- 35 132 J. L. Schrenk, M. C. Palazzotto and K. R. Mann, *Inorg. Chem.*, 1983, **22**, 4047–4049.
- 133 D. A. Freedman, J. R. Matachek and K. R. Mann, *Inorg. Chem.*, 1993, **32**, 1078–1080.
- 134 M. A. Bennett and A. K. Smith, *J. Chem. Soc. Dalton Trans.*, 1974, 233–241.
- 135 T. Hayashida and H. Nagashima, *Organometallics*, 2002, **21**, 3884–3888.
- 40 136 D. A. Loginov, M. M. Vinogradov, Z. A. Starikova and A. R. Kudinov, *Russ. Chem. Bull.*, 2013, **62**, 1262–1267.
- 137 D. A. Loginov, E. V. Mutsenek, Z. A. Starikova, E. A. Petrovskaya and A. R. Kudinov, *Russ. Chem. Bull.*, 2014, **63**, 2290–2298.
- 138 C. Long, *J. Phys. Chem. A*, 2012, **116**, 6845–6850.
- 45 139 I. P. Clark, M. W. George, G. M. Greetham, E. C. Harvey, C. Long, J. C. Manton, H. McArdle and M. T. Pryce, *J. Phys. Chem. A*, 2012, **116**, 962–969.
- 140 A. G. Sergeev and J. F. Hartwig, *Science*, 2011, **332**, 439–443.

- 141 N. I. Saper and J. F. Hartwig, *J. Am. Chem. Soc.*, 2017, **139**, 17667–17676.
- 142 B. Sawatlon, T. Wititsuwannakul, Y. Tantirungrotechai and P. Surawatanawong, *Dalton Trans.*, 2014, **43**, 18123–18133.
- 143 F. Zhu and Z. X. Wang, *Adv. Synth. Catal.*, 2013, **355**, 3694–3702.
- 5 144 T. Harada, Y. Ueda, T. Iwai and M. Sawamura, *Chem. Commun.*, 2018, **54**, 1718–1721.
- 145 T. L. Gianetti, R. G. Bergman and J. Arnold, *Chem. Sci.*, 2014, **5**, 2517–2524.
- 146 N. C. Tomson, J. Arnold and R. G. Bergman, *Dalton Trans.*, 2011, **40**, 7718–7729.
- 147 R. P. Houghton, M. Voyle and R. Price, *J. Chem. Soc. Chem. Commun.*, 1980, 884–885.
- 148 R. P. Houghton, M. Voyle and R. Price, *J. Chem. Soc. Perkin Trans. 1*, 1984, 925–934.
- 10 149 M. Otsuka, K. Endo and T. Shibata, *Chem. Commun.*, 2010, **46**, 336–338.
- 150 M. Otsuka, H. Yokoyama, K. Endo and T. Shibata, *Synlett*, 2010, 2601–2606.
- 151 A. I. Konovalov, E. O. Gorbacheva, F. M. Miloserdov and V. V. Grushin, *Chem. Commun.*, 2015, **51**, 13527–13530.
- 152 T. Tsuchimoto, M. Iwabuchi, Y. Nagase, K. Oki and H. Takahashi, *Angew. Chem. Int. Ed.*, 2011, **50**, 1375–1379.
- 15 153 K. Yonekura, Y. Yoshimura, M. Akehi and T. Tsuchimoto, *Adv. Synth. Catal.*, 2018, **360**, 1159–1181.
- 154 K. Yonekura, M. Shinoda, Y. Yonekura and T. Tsuchimoto, *Molecules*, 2018, **23**, 838–855.
- 20 155 D. Astruc, J. R. Hamon, E. Roman and P. Michaud, *J. Am. Chem. Soc.*, 1981, **103**, 7502–7514.
- 156 S. Takemoto, E. Shibata, M. Nakajima, Y. Yumoto, M. Shimamoto and H. Matsuzaka, *J. Am. Chem. Soc.*, 2016, **138**, 14836–14839.
- 157 M. Utsunomiya and J. F. Hartwig, *J. Am. Chem. Soc.*, 2004, **126**, 2702–2703.
- 25 158 J. Takaya and J. F. Hartwig, *J. Am. Chem. Soc.*, 2005, **127**, 5756–5757.
- 159 M. Otsuka, H. Yokoyama, K. Endo and T. Shibata, *Org. Biomol. Chem.*, 2012, **10**, 3815–3818.
- 160 J. M. O’Connor, S. J. Friese and B. L. Rodgers, *J. Am. Chem. Soc.*, 2005, **127**, 16342–16343.
- 30 161 T. P. Lockhart, P. B. Comita and R. G. Bergman, *J. Am. Chem. Soc.*, 1981, **103**, 4082–4090.

<sup>a</sup> Durham University, Department of Chemistry, Lower Mountjoy, Durham, DH1 3LE; E-mail: james.walton@durham.ac.uk

<sup>b</sup> Department of Chemistry, Imperial College London, London, SW7 2AZ; E-mail: l.wilkinson@imperial.ac.uk